Spring 1-1-2013

The Effects of Iron on Optical Properties of Dissolved Organic Matter

Brett Albert Poulin
University of Colorado at Boulder, poulinbrett@gmail.com

THE EFFECTS OF IRON ON OPTICAL PROPERTIES OF DISSOLVED ORGANIC MATTER

By

BRETT ALBERT POULIN

B.S., University of California Santa Cruz, 2008

A thesis submitted to the

Faculty of the Graduate School of the

University of Colorado in partial fulfillment

Of the requirement for the degree of

Masters of Science

Department of Civil, Environmental, and Architectural Engineering

2013

This thesis entitled:

The Effects of Iron on Optical Properties of Dissolved Organic Matter

written by Brett Albert Poulin

has been approved for the Department of Civil, Environmental, and Architectural Engineering

_____

Dr. Joseph N. Ryan

_____

Dr. George R. Aiken

Date_____

The final copy of this thesis has been examined by the signatories, and we
Find that both the content and the form meet acceptable presentation standards
Of scholarly work in the above mentioned discipline.

ABSTRACT

The effects of iron on optical properties of dissolved organic matter

Written by Brett Albert Poulin (M.S., Civil, Environmental, and Architectural Engineering)

Thesis directed by Professor Joseph N. Ryan

Although iron is a recognized source of spectroscopic interference in the analysis of dissolved organic matter (DOM), its effects on the absorption and fluorescence of DOM are poorly defined. Here, iron(II) and iron(III) titration experiments (0 – 1.5 mg L^{-1}) were performed with two DOM isolates and two surface water samples collected from environments spanning a range of DOM source materials. Changes in DOM UV-vis absorption and fluorescence properties were characterized. The effects of iron(II) on DOM UV-vis absorption coefficients were negligible. Additive effects of iron(III) on DOM UV-vis absorption coefficients were observed for all samples independent of DOM composition. Iron(III) extinction coefficients were established at prominent UV-vis wavelengths utilized for DOM characterization. Consequently, UV-vis absorption by iron(III) increased the measured specific UV absorbance at λ = 254 nm ($SUVA_{254}$) and decreased the measured spectral slope ratio (S_R) and absorption ratio at λ = 250 to 365 nm (E_2:E_3) of all DOM samples. In contrast, both iron(II) and iron(III) quenched the fluorescence of the DOM isolates and surface water samples at pH 6.7. The degree and location of fluorescence quenching varied with the iron:DOC ratio and between DOM source materials. Regions of the fluorescence excitation-emission matrix (EEM) spectra associated with greater DOM conjugation were found to be more susceptible to iron quenching, and DOM fluorescence indices were sensitive to the presence of iron. The analysis of EEMs using a 7- and 13-component parallel factor analysis (PARAFAC) model showed low PARAFAC sensitivity to iron addition. Acidification of samples to pH ≤ 3 minimized quenching by iron.

Acknowledgements

I'd like to acknowledge Kenna D. Butler, Blaine R. McCleskey, Benjamin Kamark, Katie Merriman, and Chase Gerbig for assistance with sample collection, sample analysis and data processing.

TABLE OF CONTENTS

INTRODUCTION 1

EXPERIMENTAL METHODS 4

MATERIALS 4

IRON TITRATIONS 5

SAMPLE ANALYSIS 6

RESULTS 10

DOM PROPERTIES 10

IRON OXIDATION STATE OF EXPERIMENTAL SOLUTIONS 11

IRON COLLOID FORMATION 12

EFFECTS OF IRON ON DOM UV-VIS ABSORPTION 13

EFFECTS OF IRON ON DOM FLUORESCENCE AT pH 6.7 18

pH EFFECT ON IRON QUENCHING OF SUWANNEE RIVER HPoA 24

DISCUSSION 28

IRON OXIDATION STATE OF EXPERIMENTAL SOLUTIONS 28

IRON COLLOID FORMATION 29

EFFECTS OF IRON ON DOM UV-VIS ABSORPTION 29

EFFECTS OF IRON ON DOM FLUORESCENCE 33

CONCLUSIONS AND IMPLICATIONS 38

REFERENCES 41

APPENDIX 45

LIST OF TABLES

Table 1. Optical properties of DOM isolates and surface water samples..... 10

Table 2. Iron(III) extinction coefficients..... 16

Table A-1. Ion and metal concentrations of surface water samples and DOM isolates..... 45

Table A-2. Iron(III) concentration thresholds for UV-vis absorption measurements. 46

Table A-3. PARAFAC modeling results of Suwannee River HPoA between pH 2 – 6.7 in the presence and absence of iron. 47

LIST OF FIGURES

Figure 1. Distribution of iron oxidation state of systems equilibrated at pH 2 – 6.7 12

Figure 2. Effects of iron(III) on decadic absorption coefficients at λ = 254 nm 14

Figure 3. UV absorption spectra of iron(III)-DOM systems. 15

Figure 4. DOM absorption coefficients at λ = 254 nm corrected for iron(III). 17

Figure 5. Relative fluorescence of DOM samples in the presence of iron 19

Figure 6. Surface water sample EEMs of fluorescence quenched by iron(II) 21

Figure 7. Effects of iron(II) on fluorescence emission 370 nm and fluorescence index 23

Figure 8. pH effects on Suwannee River HPoA fluorescence in the absence and presence of iron. 25

Figure 9. pH effects on Suwannee River HPoA EEMs 26

Figure A-1. UV-vis absorption spectra of iron(III)-DOM systems equilibrated between 0.5 – 96 h 48

Figure A-2. EEMs of DOM samples 49

Figure A-3. Relative changes in Rayleigh scattering of pH 6.7 systems 51

Figure A-4. Rayleigh scattering of systems equilibrated at pH 2 – 6.7 52

Figure A-5. Effects of iron(III) on spectral slope ratio and E_2:E_3 ratio 54

Figure A-6. HPoA sample EEMs of fluorescence quenched by iron(II). 56

Figure A-7. EEMs of fluorescence quenched by iron(III) of all samples 57

Figure A-8. pH effect on 2D fluorescence emission spectra in the presence and absence of iron 58

Figure A-9. pH effects on fluorescence indices in the presence and absence of iron. 60

CHAPTER 1

INTRODUCTION

The importance of dissolved organic matter (DOM) on biogeochemical, ecological, and engineering processes has been well-studied over the last three decades. For example, DOM quantity and quality are known to exert control on the fate and transport of trace metals (Aiken et al., 2011), biogeochemical redox reactions (Aeschbacher et al., 2012), and the formation of disinfection byproducts during water treatment (Weishaar et al., 2003). UV-vis absorption and fluorescence optical measurements have emerged as an important analytical approach to characterize DOM across a range of environmental disciplines (Chin et al., 1994; McKnight et al., 2001; Weishaar et al., 2003; Cory and McKnight, 2005; Helms et al., 2008). However, iron can be present at parts-per-million concentrations in ground and surface waters, and a careful survey of the literature identifies numerous studies recognizing iron as a source of spectroscopic interference for DOM UV-vis absorption (Meier et al., 1999; Bertilsson and Tranvik, 2000; Weishaar et al., 2003; Maloney et al., 2005; Doane and Horwáth, 2010) and fluorescence measurements (Waite and Morel, 1984; Senesi, 1990; Cabaniss, 1992; McKnight et al., 2001; Pullin et al., 2007). Despite these observations, a comprehensive laboratory study evaluating and quantifying these interferences on long-standing and novel optical techniques has yet to be performed.

Aqueous iron(III) complexes (Stefánsson, 2007) as well as colloidal iron (Pullin and Cabaniss, 2003) have been observed to absorb light in UV regions historically utilized to characterize bulk DOM properties including molecular weight (Chin et al., 1994) and aromatic carbon content (Weishaar et al., 2003). UV-vis parameters like the specific UV absorbance at λ = 254 nm ($SUVA_{254}$) (Weishaar et al., 2003), defined as the UV absorbance at λ = 254 nm normalized to the dissolved organic carbon (DOC) concentration, serve as a proxy for DOM aromaticity and are therefore subject to uncertainties in the presence of iron(III). Doane and Horwáth (2010) recently demonstrated the elimination of iron(III)

interference by chemically reducing iron(III) to nonabsorbing iron(II). However, the proposed method relies on UV-vis spectra correction for the reductant, raises questions regarding potential irreversible transformation to DOM chemical properties (Maurer et al., 2010), and does not provide a means to correct previously acquired or archived data. For these reasons, an alternative empirical iron(III) correction protocol is desirable.

In contrast to UV-vis interferences, DOM fluorescence is known to be quenched (i.e., reduced) by static interactions with paramagnetic metal ions (Plaza et al., 2006; Yamashita and Jaffé, 2008) including iron(III) (Senesi, 1990; Cabaniss, 1992; Ohno et al., 2007; Pullin et al., 2007). Specifically, ground state metal-DOM complexes enhance intersystem crossing and other non-radiative processes that compete with DOM fluorescence (Senesi, 1990; Lakowicz, 2006). Previous fluorescence quenching studies highlight that the degree of quenching can vary by spectral region (Cabaniss, 1992) based on DOM compositional differences (Plaza et al., 2006; Pullin et al., 2007). These observations are of importance because qualitative fluorescence parameters relate the relative fluorescence of one peak or region to another (McKnight et al., 2001; Stedmon et al., 2003; Cory and McKnight, 2005). Thus, elevated levels of iron may represent a significant and unpredictable source of interference in determining fluorescence parameters, such as the fluorescence index (FI) (McKnight et al., 2001), commonly used to infer DOM source. Multiple studies have additionally noted variance in DOM fluorescence (Mobed et al., 1996; Spencer et al., 2007) and iron-quenching efficiency (Waite and Morel, 1984; Cabaniss, 1992) over large swings in pH. In the latter case, iron(III) colloids formed at circumneutral pH were less effective at quenching when compared with samples equilibrated at mildly acidic pH. Investigators have acidified samples (pH 2) to minimize metal quenching via metal complex dissociation (McKnight et al., 2001); however, this has yet to be verified in a laboratory setting. Lastly, the elevated levels of iron(II) common in subsurface and well-oxygenated surface waters (Gaffney et al., 2008) warrant investigation of fluorescence quenching by iron(II). A summary of results from past

studies present an unresolved relationship between iron oxidation state, iron colloid formation, pH and fluorescence interferences.

In this study, iron(II) and iron(III) titration experiments were performed on two DOM isolates and two surface water samples collected from a variety of environments differing in DOM origin. UV-vis and fluorescence measurements were made on iron-DOM equilibrated systems. This work sought to establish an empirical UV-vis iron(III) correction protocol, outline iron(III) thresholds for UV-vis absorption measurements, and characterize changes in prominent parameters including $SUVA_{254}$, spectral slope ratio (S_R) (Helms et al., 2008) and absorption ratio at λ = 250 to 365 nm (E_2:E_3) (De Haan and De Boer, 1987). Fluorescence efforts aimed to identify regions of excitation-emission matrix (EEM) fluorescence quenched by iron across a range of DOM source material, assess the sensitivity of a 7-component (Cawley et al., 2012) and 13-component parallel factor analysis (PARAFAC) model (Cory and McKnight, 2005) to iron interferences, and quantify changes in prominent fluorescence indices. Additionally, pH effects on DOM fluorescence in the presence and absence of iron were evaluated using a well-characterized DOM isolate.

CHAPTER 2

EXPERIMENTAL METHODS

MATERIALS

DOM isolation was performed according to the method outlined by Aiken et al. (1992) on water samples collected from the Suwannee River (GA) (01/1996) and Everglades F1 site (FL) (08/2010). Hydrophobic acid (HPoA) isolate fractions were used in this study, and encompass both humic and fulvic acid fractions. Surface water samples were collected in the Everglades F1 site (FL) (08/18/2010) and Williams Lake (MN) (09/08/2010), filtered (0.45 µm capsule filter; Geotech Environmental Equipment Inc.) and refrigerated until use (≤ 16 d after collection). The Everglades F1 HPoA sample was isolated from the Everglades F1 surface water sample used in this study. Surface water samples from the Everglades F1 site (FL) and Williams Lake (MN) had original DOC concentrations of 25.01 and 7.46 $mg_C\ L^{-1}$, and were diluted with deionized (DI) water (≥ 18MΩ cm resistivity) to final DOC concentrations of 5.00 and 4.50 $mg_C\ L^{-1}$, respectively. Estimates of electron-donating capacity of Suwannee River HPoA and Williams Lake water are outlined in the Appendix using published values of International Humic Substances Society (IHSS) isolates (Aeschbacher et al., 2012). All other reagents were purchased from either Fisher Scientific or Acros Organics. All acids were trace metal-grade.

Iron stock solutions (10 mM) were prepared by dissolving $Fe_2(SO_4)_3(H_2O)_5$ and $FeSO_4(H_2O)_7$ in 1 N HCl. The concentration of iron stock solutions were verified by inductively coupled mass optical emission spectroscopy (ICP-OES; ARL 3410+).The oxidation state of iron stock solutions were verified at > 99% that of added salts by ferrozine analysis (To et al., 1999). DOM stock solutions (50 $mg_C\ L^{-1}$) were prepared by dissolving DOM isolates in DI water and passing through a 0.45 µm Supor® membrane syringe filter (Pall Corporation). All glassware used in sample preparation was I-Chem 200 series

borosilicate glass jars (Fisher Scientific) with Teflon®-lined caps. Glassware was acid cleaned (solution of 10% HCl and 10% HNO_3) and baked at 450° C for 4 h to remove trace organic compounds.

IRON TITRATIONS

Stock and experimental solutions were prepared in a anaerobic glove box (filled with 5% H_2, 95% N_2; Coy Laboratory Products Inc.) with de-aired DI water to minimize changes in the oxidation state of added iron and eliminate O_2 as a dynamic fluorescence quenching agent (Lakowicz, 2006). All solution vessels and light-sensitive stock solutions were covered with aluminum foil. DI water and dilute surface water samples were de-aired by purging with ultra-high purity He for 1 h. Experimental solutions were prepared in duplicate at pH 6.7 and allowed to equilibrate for 24±4 h at room temperature. Tests showed no significant change in absorption spectra (≤ 2% at wavelengths above 220 nm) of Suwannee River HPoA (2.49 $mg_C\ L^{-1}$) equilibrated with 1.5 mg L^{-1} iron(III) between 4 and 96 h (Figure A-1). Additional iron solubility tests were performed on identical 24 h-equilibrated solutions. Solutions were passed through a 0.45 µm Supor® Membrane syringe filter (Pall Corporation) and analyzed for total iron, [DOC], $SUVA_{254}$, and fluorescence properties. Filtration had no significant effect (≤ 1%) on analyte concentrations or DOM spectroscopic measurements. An operation cutoff of 0.45 µm was chosen due to its wide acceptance for the collection of field samples. Experimental conditions were designed such that the absorbance at λ = 254 nm (A_{254}) < 0.2 cm^{-1} to minimize inner filter effects during fluorescence analysis (Mobed et al., 1996; McKnight et al., 2001). Experimental solutions were prepared with a 0.01 M $NaHCO_3$ buffer to minimize changes in pH and iron(II) oxidation by autocatalysis from iron(III) (hydr)oxide particles (Pullin and Cabaniss, 2003). In solutions containing DOM isolates, DOM was added from stock solutions to bring the DOC concentration to approximately 2.5 $mg_C\ L^{-1}$. In surface water containing solutions, reagents were added to previously diluted waters (described above in Materials).

The addition of iron stock solutions resulted in an iron concentration range of 0 – 1.5 mg L^{-1}, and solutions were immediately adjusted to pH 6.7±0.2 with 0.1 M NaOH and 0.1 N HCl. Sample cuvettes were filled in the anaerobic glove box, capped and brought out for immediate spectroscopic analysis.

Additional iron(II) titrations were conducted in the absence of carbonate with Suwannee River HPoA at seven pH values between 2 – 6.7 to assess (1) UV interferences by iron(III) formed via iron(II) oxidation and (2) pH dependence of iron quenching. All experimental solutions were prepared in experimental duplicate and contained 1 mM $NaClO_4$ and 2.48 mg_C L^{-1} DOC. Control solutions were prepared at each pH value (± 0.2) with no added iron. Experimental solutions containing iron were spiked with 0.68 mg L^{-1} iron(II). After addition of iron stock solutions, sample pH was immediately adjusted with 0.1 N HCl and 0.1 M NaOH to their target pH (± 0.2). Solution pH was re-adjusted after 2 h equilibration time due to consequent changes in pH from iron(II) oxidation. All samples, excluding pH 2 treatments, deviated in ionic strength by < 10% (Visual MINTEQ version 3.0; Gustafsson, 2011). Tests concluded that the adjustment of solution ionic strength to 1 mM (equivalent to the ionic strength of pH 3 – 6.7 treatments) and 10 mM (equivalent to the ionic strength of pH 2 treatment) with $NaClO_4$ did not alter Suwannee River HPoA spectroscopic properties.

SAMPLE ANALYSIS

Measurements of pH (Beckman Coulter pHi410), total iron, and iron(II) were performed within 3 h of spectroscopic analysis of sample solutions inside the oxygen-free chamber. Total iron and iron(II) levels (mg L^{-1}) were measured using Hach Ferrover® AccuVac® ampules and Ferrous AccuVac® ampules with a Hach DR2700 spectrophotometer. Iron(III) concentrations were determined as the difference between total iron and iron(II). Periodically, samples were preserved with 1% volume/volume 6 N HCl and total iron and iron(II) levels were confirmed by a ferrozine assay (To et al., 1999). Results showed

adequate agreement between the two iron determination methods (difference between methods ≤ 0.02 mg L^{-1}). DOC concentrations were determined by perchlorate oxidation using a total organic carbon analyzer (Oceanographic Instrument Analytical, Oceanographic Instrument 700).

UV-vis absorption spectra from 190 – 800 nm were obtained using a UV-vis spectrophotometer (Agilent Technologies, model 8453) using a 1 cm quartz cuvette. The UV-vis spectrophotometer was blanked with DI water prior to spectra collection. Decadic absorbance values were converted to absorption coefficients as follows:

$$a_{(\lambda)} = \frac{A_{(\lambda)}}{l} \quad (1)$$

where $a_{(\lambda)}$ is the absorption coefficient (cm^{-1}), $A_{(\lambda)}$ is the absorbance, and l is the path length (cm). $SUVA_{254}$ values were calculated by dividing the decadic a_{254} to [DOC] and are reported in units of L mg_C^{-1} m^{-1} (Weishaar et al., 2003). The E_2:E_3 is defined as the ratio of decadic a_{250} to a_{365}, and shows an inverse correlation with DOM molecular size (De Haan and De Boer, 1987). For measurements of spectral slope, Naperian absorption coefficients were determined using the following:

$$\alpha_{(\lambda)} = \frac{2.303A_{(\lambda)}}{l} \quad (2)$$

where $\alpha_{(\lambda)}$ is the Naperian absorption coefficient (cm^{-1}), $A_{(\lambda)}$ is the absorbance, and l is the path length (cm). The spectral slope was calculated by fitting the exponential equation 3 to the Naperian absorption spectra between wavelengths of 275 – 295 nm ($S_{275\text{-}295}$) and 350 – 400 nm ($S_{350\text{-}400}$):

$$\alpha_{g(\lambda)} = \alpha_{g(\lambda_{ref})} e^{-S(\lambda - \lambda_{ref})} \quad (3)$$

where $\alpha_{g(\lambda)}$ is the absorption coefficient at the specified wavelength, $\alpha_{g(\lambda_{ref})}$ is the absorption coefficient at the reference wavelength, and S is the slope fitting parameter (Helms et al., 2008). The spectral slope ratio (S_R) was defined as $S_{275\text{-}295} : S_{350\text{-}400}$ and has been inversely correlated to DOM

molecular weight (Helms et al., 2008). In determining iron(III) extinction coefficients (ε_λ), decadic absorption coefficients measured at pH 6.7 were first corrected for the known absorption coefficients of DOM samples. The linear regression (i.e., Beer's Law) between corrected decadic absorption coefficients (cm^{-1}) and iron(III) concentration (mg L^{-1}) were used to generated ε_λ and are presented in L mg^{-1} cm^{-1}. The y-intercept (a_λ) of linear regressions at 254, 280, and 400 nm were all less than or equal to the instrument background absorption coefficient (2 x 10^{-3} cm^{-1}).

Fluorescence EEMs were collected by scanning samples between excitation 240 – 450 nm at 5 nm intervals and emission 300 – 600 nm at 2 nm intervals with a fluorometer (Jobin Yvon Horiba , Fluoromax 3). Fluorescence spectra were corrected for UV-vis absorption, DI blank, Raman scatter, and background system constituents (e.g., 0.01 M $NaHCO_3$ at pH 6.7) and are presented in Raman units (RU). The overall fluorescence intensity (OFI) was generated by addition of all fluorescence signals across the entire range of excitation wavelengths. The Rayleigh scatter, a measurement of intra-molecular light scatter, was determined at excitation/emission 350/350 nm (Ohno et al., 2007). Due to differences in quantum yield between DOM samples, comparisons between DOM fluorescence data for different iron concentrations determined at pH 6.7 are presented as the relative fluorescence (OFI/OFI_o), with OFI and OFI_o being in the presence and absence of iron, respectively. Changes in DOM fluorescence were observed for both iron(II) and iron(III) titrations; therefore, total iron concentrations were used to determine iron:DOC ratios even though changes in iron oxidation were observed (see results below). The fluorescence index (FI) was determined using two prominent fluorescence emission ratios of 470 to 520 nm (Cory and McKnight, 2005) and 450 to 500 nm (McKnight et al., 2001) at excitation 370 nm. EEMs were analyzed using two PARAFAC models. The 7-component model was developed using 270 EEMs collected on filtered surface water samples following the Androscoggin and Penobscot rivers to the Gulf of Maine (Cawley et al., 2012). The 13-component model was developed using 379 EEMs collected from (1) filtered surface water samples, (2) ultrafiltered DOM, and (3) fulvic and hydrophobic

acid DOM isolate fractions from a variety of environments (Cory and McKnight, 2005). The residual from PARAFAC modeling results was determined as the difference between collected and modeled EEMs and was always below 10% of the original spectra. EEM subtractions were conducted using MATLAB® (version R2008b) to generate a positive representation of the fluorescence quenched (EEM_{FQ}) upon iron addition using the following:

$$EEM_{FQ} = EEM_o - EEM \quad (4)$$

where EEM_o and EEM were in the absence and presence of iron, respectively. Similarly, EEMs of fluorescence reduction (EEM_{FR}) upon acidification of Suwannee River HPoA in the absence of iron were determined using the following:

$$EEM_{FR} = EEM_{pH\ 6.7} - EEM_{pH} \quad (5)$$

where $EEM_{pH\ 6.7}$ was at pH 6.7 and EEM_{pH} was at the specified pH. These analyses were not performed for analogous samples in the presence of iron due to variance in iron oxidation state and pH between experimental replicates. EEM_{FQ} and EEM_{FR} were excluded from PARAFAC analysis.

CHAPTER 3

RESULTS

DOM PROPERTIES

Table 1 presents optical properties of DOM isolates and surface water samples at the given DOC concentration in the absence of iron. The range of $SUVA_{254}$, FI, and S_R values indicates that the samples in this study span a wide range of DOM composition and source materials (McKnight et al., 2001; Weishaar et al., 2003; Helms et al., 2008). EEMs of these four samples can be found in the Appendix (Figure A-2). Additional information on aqueous ion and metal concentrations of experimental solutions are presented in Table A-1.

Table 1. Optical properties of DOM isolates and surface water samples in the absence of iron at the specified DOC concentration.

	Suwannee River HPoA (GA)	**Everglades F1 HPoA (FL)**	**Everglades F1 Water (FL)**	**Williams Lake Water (MN)**
[DOC] $mg_C\ L^{-1}$	2.49	2.30	5.00	4.50
$SUVA_{254}$ ($L\ mg_C^{-1}\ m^{-1}$)	4.49	4.40	3.45	1.17
FI[a]	1.17	1.26	1.35	1.49
S_R [b]	0.67	0.86	1.02	1.53

[a]defined as the fluorescence emission 470/520 nm at excitation 370 nm (McKnight et al., 2001).
[b]defined as the $S_{275\text{-}295}$:$S_{350\text{-}400}$ (Helms et al., 2008).

IRON OXIDATION STATE IN EXPERIMENTAL SOLUTIONS

Changes in iron oxidation state from added iron stock solutions were observed in experimental solutions. In pH 6.7 systems, changes in iron oxidation state were most substantial in solutions with low iron(III) levels (0.11 mg L^{-1}), in which as much as 0.05 mg L^{-1} (≤ 45%) of added iron(III) was reduced to iron(II). The maximum observed levels of iron(III) reduction varied between DOM sample solutions, and was observed at iron(III) concentrations greater than 0.11 mg L^{-1}. However, iron(III) reduction never exceeded 0.07 mg L^{-1} in any sample. The majority of pH 6.7 solutions with added iron(II) showed acceptable preservation of iron(II) oxidation state (> 90%). Despite changes in the oxidation state of added iron, neither a chemical reductant nor oxidant was employed due to potential irreversible transformations to DOM chemical properties (Maurer et al., 2010) and the known importance of redox status on DOM fluorescence (Klapper et al., 2002; Cory and McKnight, 2005). Experiments conducted at varying pH in the absence of carbonate with added iron(II) showed low levels of iron(II) oxidation at pH < 4 and considerable iron(II) oxidation at pH > 4 (Figure 1). Consequent increases in pH were observed due to iron(II) oxidation over the 24 h equilibration time. Samples prepared at pH 5 exhibited the greatest pH increase to final pH values of 6.0 and 6.3 for experimental duplicates. Due to differences in iron oxidation state and pH between experimental replicates, single data points are presented for this experiment rather than average values.

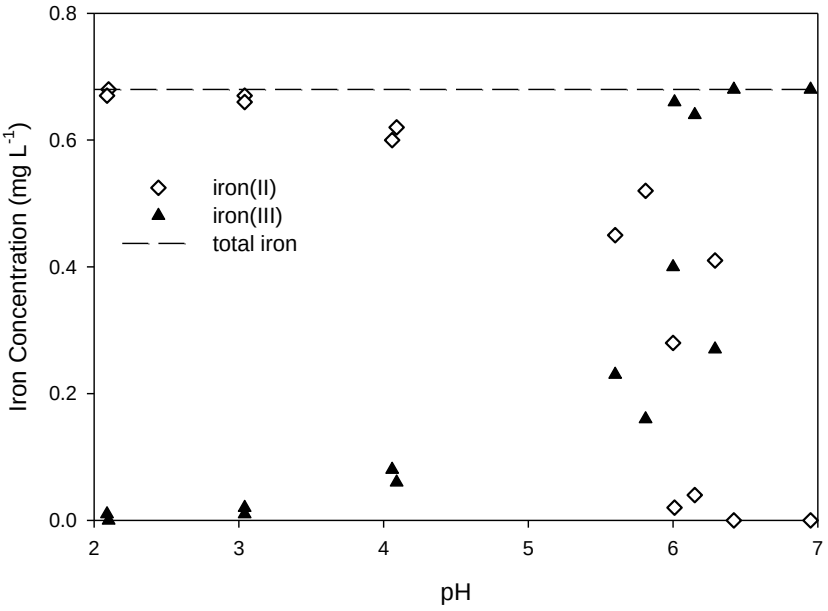

Figure 1. Distribution of iron(II) and iron(III) in solutions equilibrated for 24 h with 0.68 mg L^{-1} total iron added as iron(II) in the presence of 2.48 mg_C L^{-1} Suwannee River HPoA between pH 2 – 6.7.

IRON COLLOID FORMATION

The Rayleigh scatter of fluorescence spectra was evaluated to assess iron colloid formation in experimental solutions (Ryan and Weber, 1982; Ohno et al., 2007). Little, if any, change in Rayleigh scattering was observed in all iron(II) titrations at pH 6.7 (Figure A-3a), which is consistent with low levels of iron(II) oxidation in these samples. The Rayleigh scatter of all iron(III) titrations at pH 6.7 shows a linear increase with increasing iron(III) (Figure A-3b). Aside from the Williams Lake water, Rayleigh scattering did not exceed a two-fold increase. However, an eight-fold increase in Rayleigh scattering was observed in Williams Lake water solutions at 1.43 mg L^{-1} iron(III) (Figure A-3b). The presence of colloids in iron(III)-William Lake water samples was also noted by high background scatter of UV-vis absorption spectra; therefore, absorption and fluorescence spectra must be interpreted accordingly. In experiments

with added iron(II) at varying pH, Rayleigh scattering was low at pH < 4 and increased at pH > 4 (Figure A-4) due to iron(II) oxidation (Figure 1).

EFFECTS OF IRON ON DOM UV-VIS ABSORPTION

The effects of iron(II) on DOM absorption coefficients were negligible in all experimental solutions. Small increases in absorption coefficients observed in some samples are interpreted as artifacts due to observed iron(II) oxidation. Increasing iron(III) levels showed a positive, additive relationship with absorption coefficients at λ = 254 nm in all four DOM solutions (Figure 2a). No DOC loss was observed upon iron(III) addition. UV-vis absorption spectra of iron(III)-DOM systems showed greater iron(III) absorption at shorter UV wavelengths and an absorption decay at higher UV-vis wavelengths (example spectra presented in Figure 3a). UV-vis absorption spectra corrected for the known DOM absorption (no added iron) showed iron(III) primary and secondary absorption maxima of 206 and 271 nm (Figure 3c), which closely matched iron(III) absorption spectra collected in the absence of DOM (Figure 3c). Data in Figure 2b show a robust linear correlation (R^2 = 0.98) between iron(III) concentrations and DOM-corrected a_{254} for all DOM samples (Beer's law is obeyed), which was also observed at 280 (R^2 = 0.98) and 400 nm (R^2 = 0.88) wavelengths. From this relationship, iron(III) extinction coefficients (ε_λ) at 254, 280 and 400 nm wavelengths were determined to be 6.53 x 10^{-2}, 5.70 x 10^{-2} and 1.18 x 10^{-2} L mg^{-1} cm^{-1}, respectively (Table 2). Using extinction coefficients, the iron(III) concentration equivalent to instrumental background absorption limits (a = 2.0 x 10^{-3} cm^{-1}) were determined at 254, 280, and 400 nm (Table 2). Additionally, iron(III) concentrations thresholds were calculated that will induce a 5% increase in sample absorption coefficients (a_{254}, a_{280}, a_{400}) over a range in a_λ from 0.1 – 1.0 cm^{-1} (Table A-2).

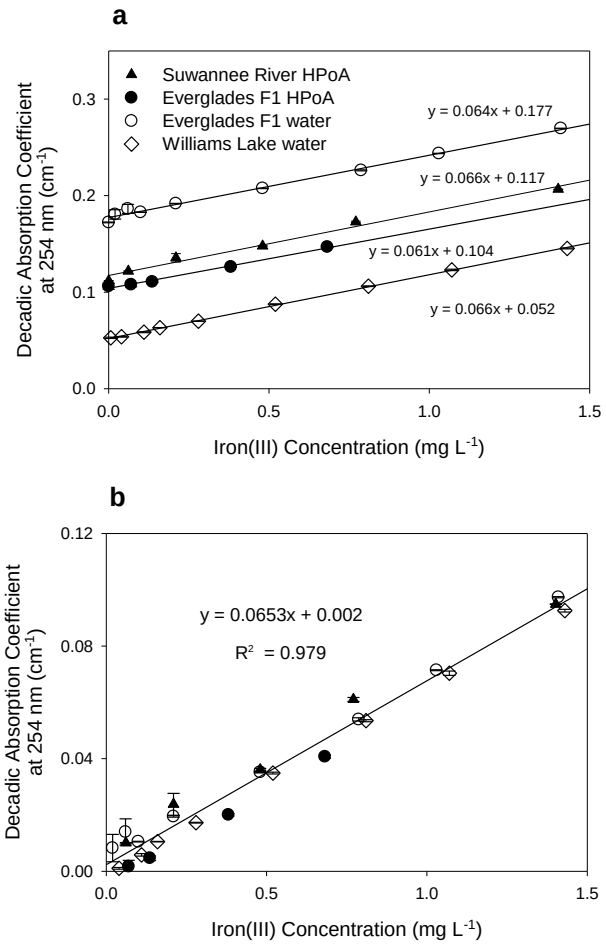

Figure 2. (a) The additive effects of iron(III) on decadic absorption coefficient at λ = 254 nm of DOM-iron(III) systems and (b) iron(III) decadic absorption coefficients at λ = 254 nm after correction for the known absorption coefficient of DOM samples. Data points are mean values of experimental duplicates with error bars indicating the high and low values observed.

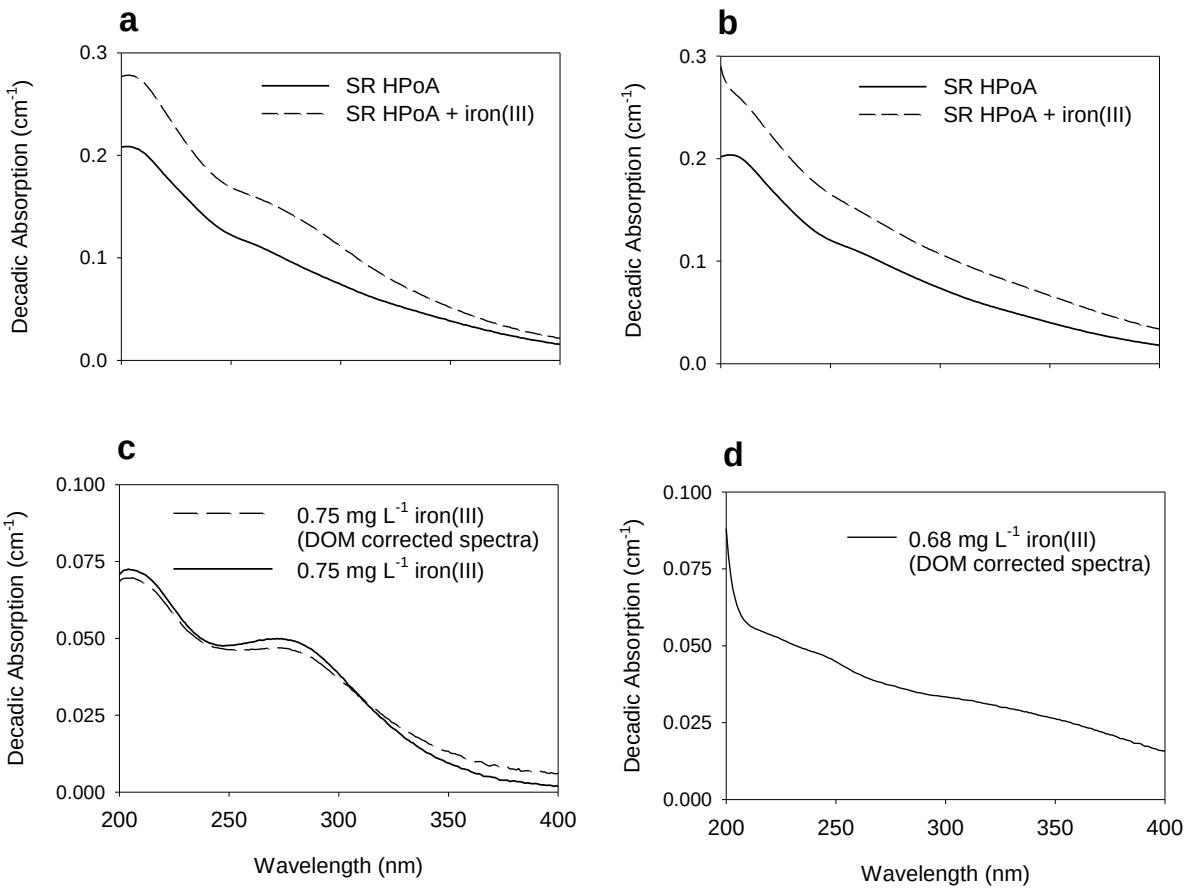

Figure 3. UV decadic absorption spectra of Suwannee River HPoA in the presence and absence of (a) 0.75 mg L^{-1} added iron(III) and (b) 0.68 mg L^{-1} iron(III) generated from iron(II) oxidation. Absorption spectra of (c) added 0.75 mg L^{-1} iron(III) collected in the presence and absence of DOM and (d) 0.68 mg L^{-1} iron(III) generated from iron(II) oxidation.

Table 2. Iron(III) extinction coefficients (ε_λ) at 254, 280 and 400 nm; R^2 and *p* values are from linear regression analysis.

Wavelength (nm)	ε_λ (L mg^{-1} cm^{-1})	*n*	R^2	*p* value	[Iron(III)] = Bkgd a_λ[a] (mg L^{-1})
254	6.53 x 10^{-2}	25	0.98	< 0.001	0.03
280	5.70 x 10^{-2}	25	0.98	< 0.001	0.04
400	1.18 x 10^{-2}	25	0.88	< 0.001	0.17

[a]denotes the iron(III) concentration (mg L^{-1}) equivalent to the instrument background absorption coefficient (2 x 10^{-3} cm^{-1}) at the given wavelength.

Greater DOM absorption coefficients due to iron(III) resulted in considerable increases in the measured $SUVA_{254}$ for all DOM samples. For example, the maximum titrated iron(III) concentration (1.43 mg L^{-1}) increased the measured Everglades F1 water $SUVA_{254}$ from 3.45 to 5.32 L mg$_C^{-1}$ m^{-1} (Δ 1.92 $SUVA_{254}$ units). However, the degree to which a given iron(III) concentration affected $SUVA_{254}$ varied between DOM samples due to differences in sample optical density and DOM molar absorptivity. Values of S_R decreased with increasing iron(III) in all four samples (Figure A-5) due to a reduction in the magnitude of $S_{275\text{-}295}$ (i.e., less negative) accompanied by relatively negligible changes in $S_{350\text{-}400}$. Values of $E_2{:}E_3$ also decreased with increasing iron(III) (Figure A-5) due to greater relative increases in a_{365} than a_{250}.

Experimental solutions prepared with iron(II) between pH 2 – 6.7 showed insignificant changes in Suwannee River HPoA absorption at pH < 4 (Figure 4) due to preservation of iron(II) oxidation state (Figure 1). Elevated absorption coefficient were observed at pH > 4 (Figure 4) due to iron(II) oxidation to iron(III) (Figure 1). In samples were iron(III) was quantified, a_{254} values were corrected for iron(III) absorption contributions determined using the ε_{254} value in Table 2 (Figure 4). This analysis was performed to determine if extinction coefficients established in systems with added iron(III) are applicable to solutions where iron(III) formed via iron(II) oxidation. The data in Figure 4 shows

reasonable agreement in a_{254} between control samples (no iron) and those corrected using ε_{254} over a range of pH values. $SUVA_{254}$ values established using iron(III)-corrected a_{254} values deviated by < 5.3% from those of control samples. Additionally, the UV-vis absorption spectra of iron(III) formed from iron(II) oxidation was determined by correcting for the Suwannee River HPoA absorption spectra (Figure 3d). Iron(III) formed from iron(II) oxidation showed less pronounced absorption maxima and broader absorption spectra (Figure 3d) than those collected from iron(III) addition (Figure 3c). For this reason, measured values of S_R and E_2:E_3 were relatively unchanged in the presence of iron(III) formed from iron(II) oxidation in comparison to control samples.

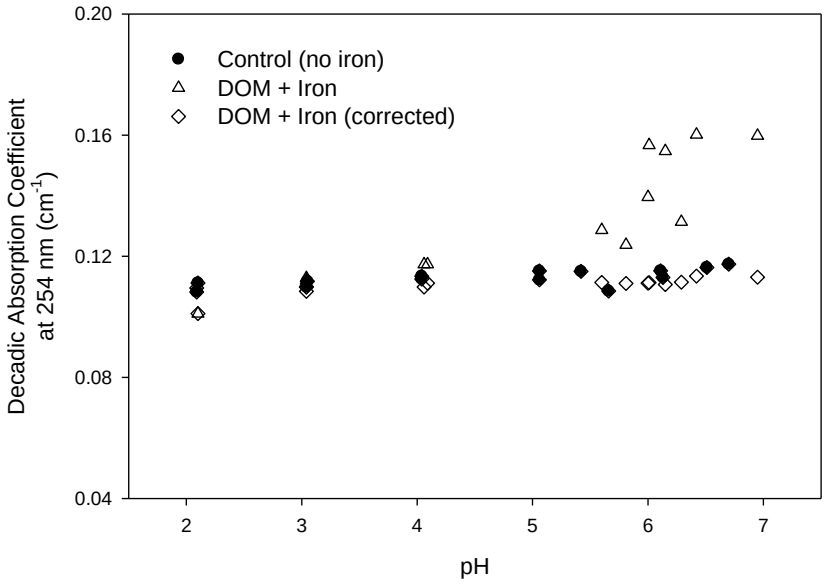

Figure 4. Decadic absorption coefficients at λ = 254 nm with varying pH of Suwannee River HPoA in the absence and presence of 0.68 mg L^{-1} iron added as iron(II). Absorption coefficients of iron containing solutions were corrected for quantified iron(III) using the reported extinction coefficient in Table 2.

EFFECTS OF IRON ON DOM FLUORESCENCE AT pH 6.7

Iron(II) addition quenched the total relative fluorescence (OFI/OFI_o) of DOM isolates and surface water samples (Figure 5a). Increasing iron(II):DOC showed a negative relationship with OFI/OFI_o for all DOM samples measured, yet the degree of fluorescence quenching varied greatly between DOM samples. For instance, the highest iron(II):DOC ratio reduced Suwannee River HPoA fluorescence by 23%, but that of Williams Lake water by only 7% (Figure 5a). The degree of fluorescence quenching of DOM samples in descending order was observed (Figure 5): Suwannee River HPoA > Everglades F1 water > Everglades F1 HPoA > Williams Lake water. Iron(III) addition resulted in comparable fluorescence quenching behavior for all samples aside from Williams Lake water, which showed quenching at low iron(III):DOC (≤ 0.06 mg_{Fe}:mg_C) and slight fluorescence enhancement at high iron(III):DOC (0.24 mg_{Fe}:mg_C; Figure 5b). The highest iron(III) titration for Williams Lake water (0.32 mg_{Fe}:mg_C) was removed from the data set due to high UV background scattering and poor reproducibility of experimental replicates. Regardless of the oxidation state of added iron, all DOM samples exhibited greater sensitivity to iron-quenching at low iron levels (Figure 5). Due to the consequent oxidation and reduction of added iron, the importance of oxidation state on iron quenching was only examined qualitatively.

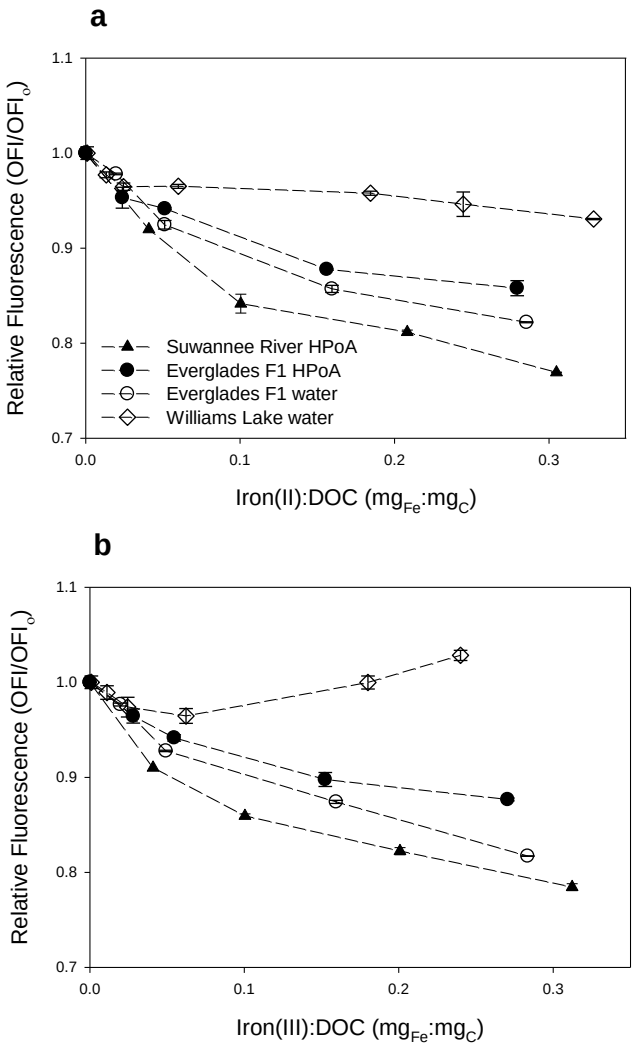

Figure 5. Relative fluorescence (OFI/OFI$_o$) of four DOM samples in the presence of (a) iron(II) and (b) iron(III). Data points are mean values of experimental duplicates with error bars indicating the high and low values observed.

EEM subtractions were performed to identify and characterize changes in quenched fluorescence (EEM$_{FQ}$) as a function of iron:DOC. Figure 6 shows the EEM$_{FQ}$ from iron(II) titrations of Everglades F1 water and Williams Lake water with increasing iron(II):DOC. The most striking feature was in Everglades F1 water samples at low iron(II):DOC (Figure 6a-b) where quenching was limited to two

EEM locations associated with humic-like fluorophores (C and A peaks; Coble, 1996). Specifically, quenching in the humic C peak region displayed an excitation/emission maxima at 365/484 nm (Figure 6a). Quenching locations shifted to include shorter excitation/emission wavelength regions with increasing iron(II):DOC (Figure 6c-d). In contrast, Williams Lake water EEM_{FQ} exhibited low levels of quenching at all iron(II):DOC ratios and no distinguishable shift in quenching regions with increasing iron(II) (Figure 6e-h). Everglades F1 HPoA experienced quenching across broad EEM regions at all iron(II):DOC ratios, while Suwannee River HPoA showed similar trends to those of Everglades F1 water as described above (Figure A-6). Aside from Williams Lake water at high iron(III):DOC, iron(III) titrations yielded similar EEM_{FQ} to those observed upon iron(II) addition and can be found in Figure A-7.

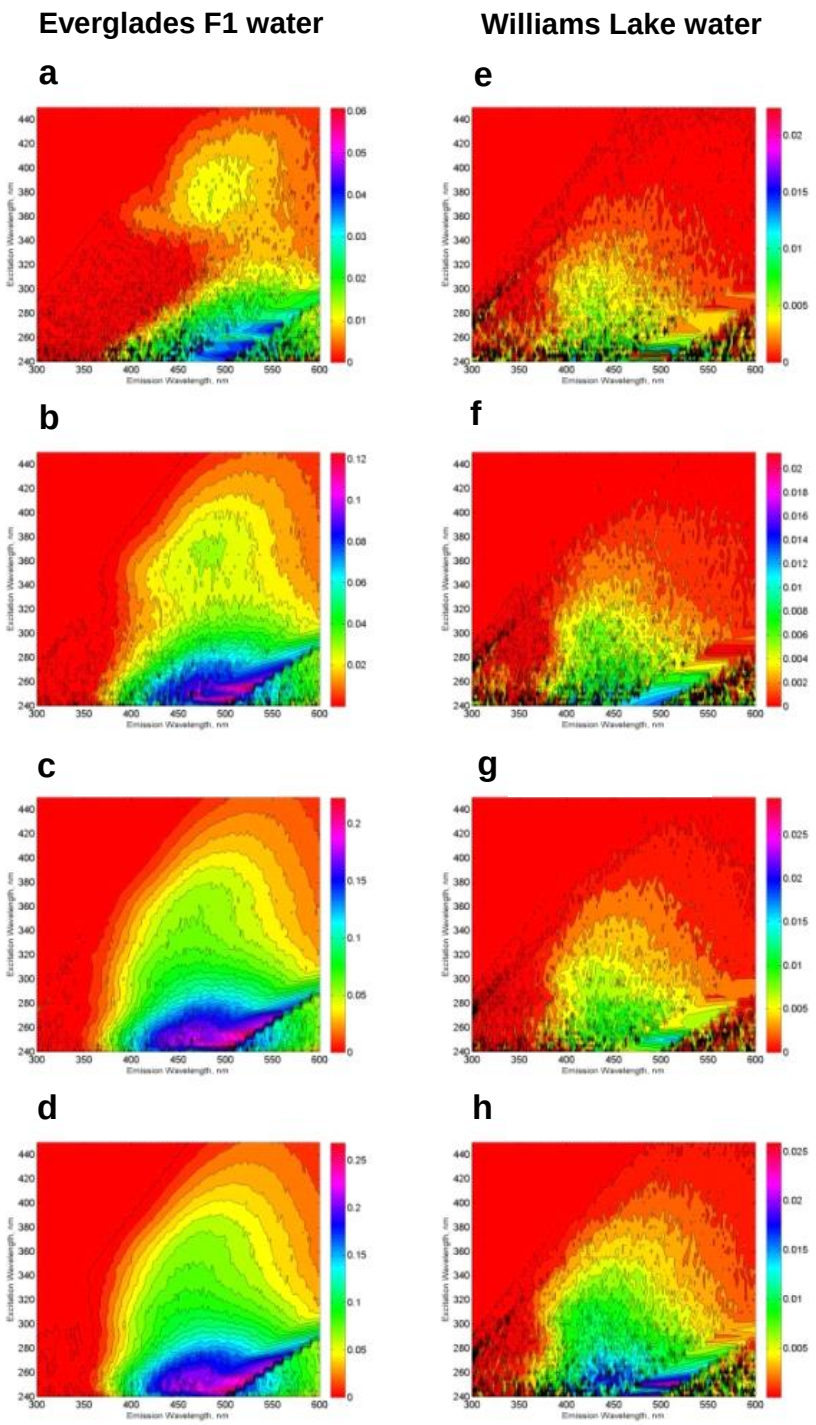

Figure 6. EEMs of fluorescence quenched (EEM_{FQ}) of Everglades F1 water at iron(II):DOC = 0.02 (a), 0.05 (b), 0.16 (c) and 0.29 mg_{Fe}:mg_C (d) and Williams Lake water at iron(II):DOC = 0.02 (e), 0.06 (f), 0.18 (g) and 0.33 mg_{Fe}:mg_C (h). All fluorescence intensities are in Raman units, and EEM_{FQ} are not normalized to the same fluorescence intensity.

Selective iron-quenching of DOM fluorescence at long excitation/emission wavelengths, as observed in Suwannee River HPoA and both Everglades F1 samples (Figure 6, A-6, A-7), increased FI values determined as the ratio of emission 470 to 520 nm at excitation 370 nm. To illustrate this, Figure 7a presents the suppression of Suwannee River HPoA fluorescence by iron(II) across excitation 370 nm with increasing iron(II):DOC. As a result, the measured FI of Suwannee River HPoA increased from 1.17 to 1.24 (change in FI (ΔFI) = 0.07) at an iron(II):DOC of 0.29 mg_{Fe}:mg_C (Figure 7b). Everglades F1 HPoA showed a similarly significant increase in FI values from 1.26 to 1.34 at high iron(II):DOC (ΔFI = 0.08), where less pronounced changes in measured fluorescence indices were observed for Everglades F1 water (ΔFI = 0.04) and Williams Lake water (ΔFI ≤ 0.02). Comparable increases in FI values were observed upon iron(III) addition, as shown for Suwannee River HPoA (Figure 7b). Fluorescence indices based on the originally proposed ratio of emission 450 and 500 nm (McKnight et al., 2001) proved slightly less susceptible to iron interference, with increases in FI ≤ 0.06 FI units across all DOM samples.

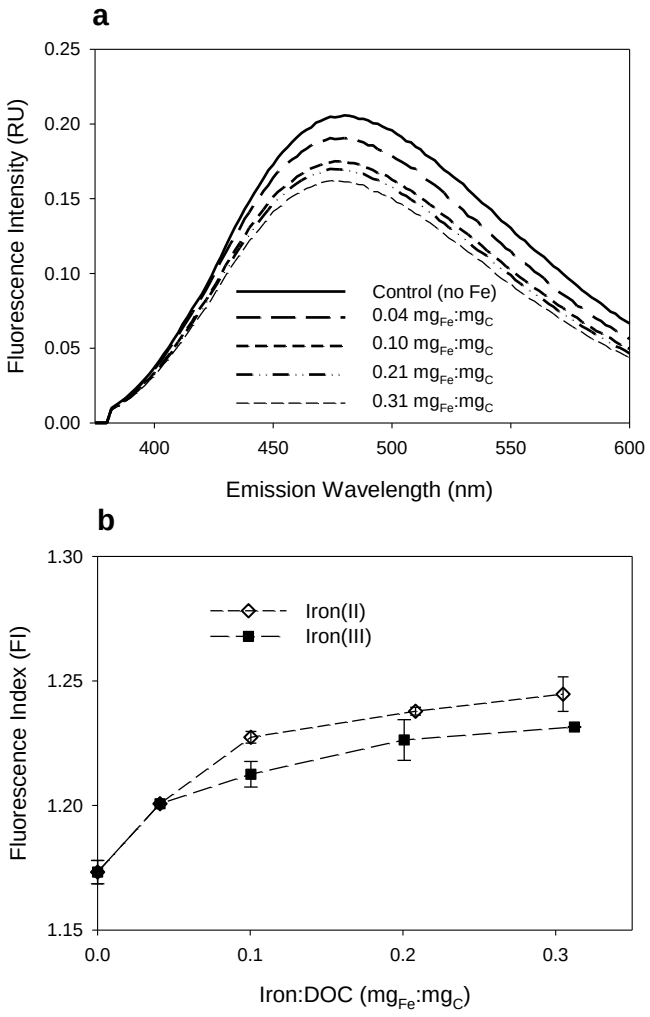

Figure 7. (a) Two-dimensional fluorescence emission 375 – 600 nm of Suwannee River HPoA iron(II) titrations at excitation 370 nm and (b) iron effects on the FI determined at emission wavelengths 470 and 520 nm at excitation 370 nm (Cory and McKnight, 2005). Data points are mean values of experimental duplicates with error bars indicating the high and low values observed.

EEMs from the iron titrations were analyzed using two PARAFAC models. Aside from the samples with the highest iron:DOC (about 0.3 mg_{Fe}:mg_C), 13-component PARAFAC modeling results did not deviate outside accepted model limitations (± 1% contribution of total fluorescence) (Cory and McKnight, 2005). When significant deviation in component distribution was observed, it was restricted to a reduction (≤ 3% of total fluorescence) in the high-molecular weight, hydrophobic (Wu et al., 2003) C4 component of HPoA samples (Cory and McKnight, 2005). More pronounced changes in PARAFAC

modeling results of Everglades F1 water and Suwannee River HPoA samples were observed using the 7-component model (Cawley et al., 2012). Everglades F1 water exhibited a decrease in C1 (≤ 3%) accompanied by an increase in C4 (≤ 2%) and C7 (≤ 3%), whereas Suwannee River HPoA showed a decrease in C3 (≤ 3%) along with an increase in C4 (≤ 3%) and C7 (≤ 2%). The reduction in the terrestrial humic C1 and C3 contributions in these samples were responsible for the increased contribution from C4 and C7 components, respectively.

pH EFFECT ON IRON QUENCHING OF SUWANNEE RIVER HPoA

Iron-free Suwannee River HPoA samples exhibited a 33% reduction in overall fluorescence intensity between pH 6.7 and 2 (Figure 8), with the greatest decrease noted between pH 3 and 2. This pH dependence was also evident in 2D fluorescence emission spectra (Figure A-8) and in EEMs of fluorescence reduction (EEM_{FR}) upon acidification (Figure 9). Specifically, fluorescence reduction was limited to long excitation/emission wavelengths (~385/475 nm) at pH 4 (Figure 9e) and included intermediate excitation/emission wavelengths at pH 3 (~305/425 nm) (Figure 9f). Relatively small changes in fluorescence indices were noted for iron free samples regardless of the emission wavelength ratio at most pH values except pH 3, where an increase in FI values was noted (Figure A-9). Suwannee River HPoA EEMs collected between pH 2 – 6.7 were analyzed using both PARAFAC models. In comparison to samples at pH 6.7, samples at pH 4 – 5 showed significant deviation (2 – 5% component distribution) for 6 components when using the 7-component PARAFAC model (Table A-3). pH 2 treatments showed no significant deviation (≤ 1% component distributions) in comparison to pH 6.7 samples. In contrast, 13-component modeling results showed less substantial deviation at pH 4-5 (3 components with ≤ 3% deviation) and considerable discrepancy at pH 2 (5 components with ≤ 3% deviation) when compared with pH 6.7 samples (Table A-3).

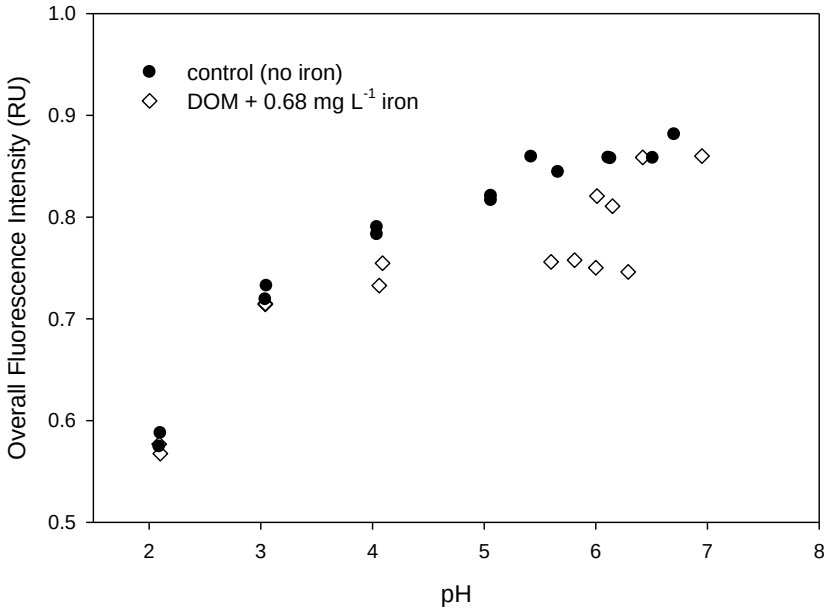

Figure 8. The overall fluorescence intensity (OFI) of Suwannee River HPoA in the absence and presence of 0.68 mg L^{-1} iron, added as iron(II), between pH 2 – 6.7.

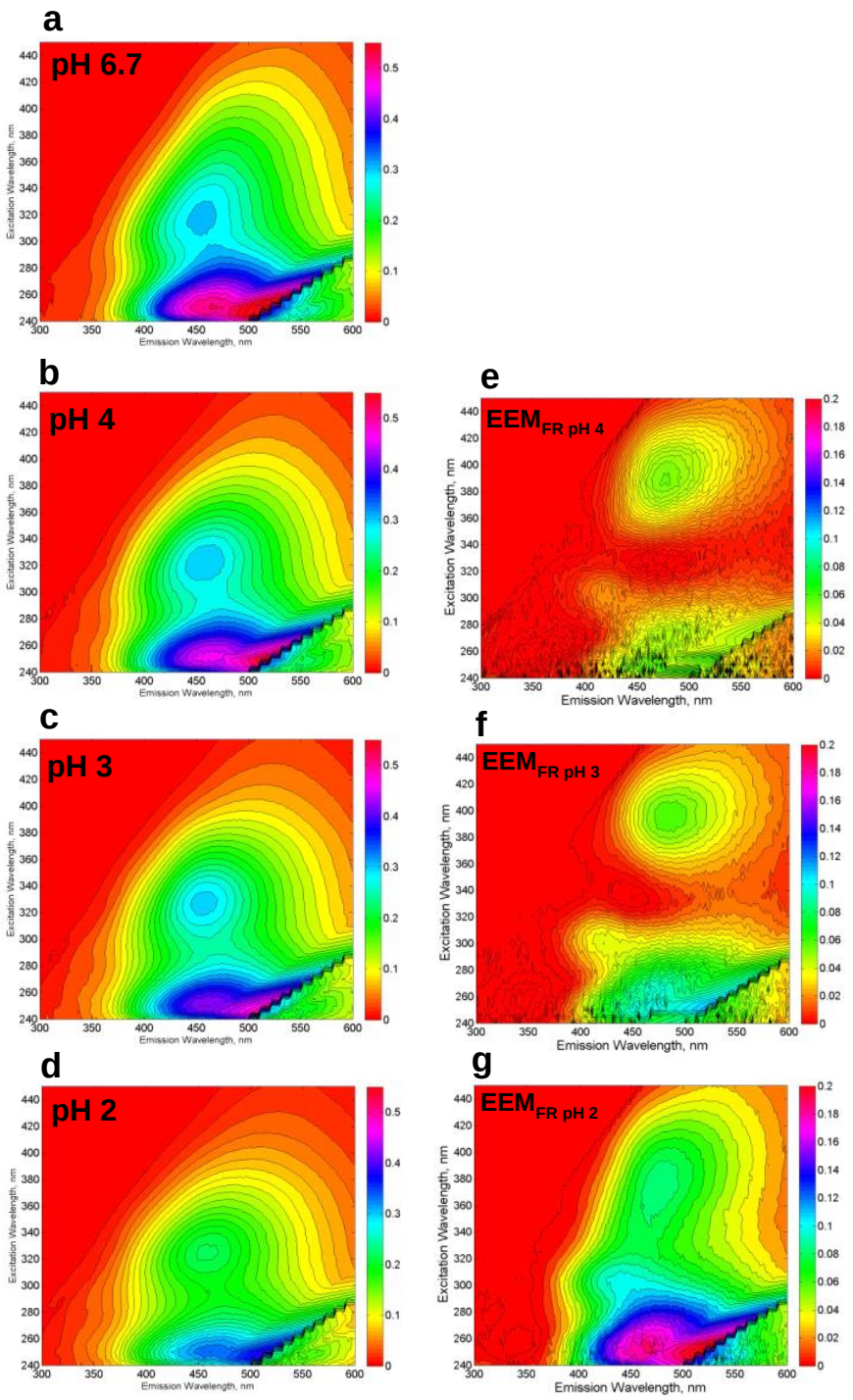

Figure 9. EEMs of Suwannee River HPoA in the absence of iron between pH 6.7 – 2 (left panel) and EEMs of fluorescence reduction (EEM_{FR}) (right panel). Fluorescence intensities are normalized for each panel.

Quenching by iron was greatest at mildly acidic pH and nearly eliminated at pH ≤ 3 and pH 6.7 (Figure 8). At pH 3, DOM fluorescence in the presence of iron as predominantly iron(II) (Figure 1) was 98% that of control samples (Figure 8). Similarly, samples prepared at pH 6.0 and 6.7 showed significant iron(II) oxidation (Figure 1) and almost no quenching (Figure 8). Samples prepared at pH 5 exhibited moderate iron(II) oxidation (Figure 1), but still showed fluorescence quenching despite the noted increase in pH. Fluorescence indices differed from those of control samples substantially at pH 4, where the FI (emission wavelength 470 and 520 nm) was 0.13 FI units greater (Figure A-9a). Changes in FI values were less pronounced when determined at emission ratio of 450 to 500 nm, but deviation from control samples as all pH values was apparent (Figure A-9b). The non-uniform reduction of Suwannee River HPoA fluorescence observed with acidification in the absence of iron (Figure 9, A-8) confounded the identification of coincident fluorescence quenching by iron. However, PARAFAC modeling results in the presence of iron largely mimicked those of control samples (Table A-3).

CHAPTER 4

DISCUSSION

IRON OXIDATION STATE OF EXPERIMENTAL SOLUTIONS

In pH 6.7 solutions, dark thermal reduction by DOM is likely responsible for the observed iron(III) reduction (Waite and Morel, 1984; Pullin and Cabaniss, 2003). The potential oxidation of DOM due to observed iron(III) reduction at pH 6.7 is discussed in detail in the Appendix. Briefly, the electron equivalent of observed iron(III) reduction was always less than 6 times the estimated electron-donating capacity of DOM samples (Aeschbacher et al., 2012). These analyses provide evidence that the oxidation of electron-donating moieties in DOM due to iron(III) reduction, predominantly phenol groups (Aeschbacher et al., 2012) recognized as prominent DOM fluorophores (Cory and McKnight, 2005), was likely insufficient to change DOM fluorescence properties. Thus, changes in DOM redox status (pH 6.7 treatments) as a function of system constituents were considered negligible. Oxidation of added iron(II) was minimal at pH 6.7 in the presence carbonate likely due to the absence of O_2 and competition by carbonate for iron(III) (hydr)oxides known to catalyze iron(II) oxidation (Pullin and Cabaniss, 2003). In contrast, Suwannee River HPoA samples prepared at pH 2 – 6.7 in the absence of carbonate showed considerable iron(II) oxidation at pH > 4 (Figure 1). Although these samples were also handled in the absence of O_2, these results suggest that iron(II) oxidation predominantly occurred through autocatalysis by iron(III) (hydr)oxides (Pullin and Cabaniss, 2003). Greater levels of iron(II) oxidation were observed at higher pH due to increased hydroxide ion concentration.

IRON COLLOID FORMATION

The formation of iron colloids from iron(III) hydrolysis, as indicated by greater Rayleigh scattering, was evident in all pH 6.7 solutions with added iron(III) (Figure A-3), and pH 6.7 – 4 Suwannee River HPoA samples with added iron(II) (Figure A-4). The lower-molecular weight, aliphatic characteristics of Williams Lake water DOM (Table 1), as opposed to the other samples, are likely responsible for greater iron(III) hydrolysis observed in this DOM sample (Pédrot et al., 2011; Jackson et al., 2012). Iron(III) (hydr)oxide precipitation at circumneutral pH is predicted based on solubility products (Stumm and Morgan, 1996), however, filter-passing concentrations in environmental samples often exceed solubility estimates due to DOM complexation and colloid stabilization (Gaffney et al., 2008). DOM is known to limit the rate (Pullin and Cabaniss, 2003) and extent (Pédrot et al., 2011) of iron(III) hydrolysis, and Gaffney et al. (2008) reported a shift to greater iron particle size distribution with increasing iron:DOC. When taken with observations from this study of differences in Rayleigh scattering between DOM samples (Figure A-3), variance in iron colloid levels and size distributions between experimental samples is likely. This phenomenon has been noted in environmental waters (Gaffney et al., 2008; Batchelli et al., 2010), which reinforces the decision to forgo extreme solution conditions (e.g., chemical reduction) to circumvent this inconsistency. Solutions equilibrated for up to 96 h showed no significant changes in UV absorption spectra (Figure A-1) suggesting that experimental systems had reached a steady state.

EFFECTS OF IRON ON DOM UV-VIS ABSORPTION

The observed negligible effects of iron(II) on DOM absorption coefficients are consistent with past findings (Doane and Horwáth, 2010). The linear relationship between iron(III) concentration and a_{254} observed across a wide range of iron:DOC, and between DOM samples (Figure 2), suggests that reported extinction coefficients are not a function of colloidal iron. This conclusion is further

substantiated by good agreement between absorption maxima of iron(III) spectra, collected in both the absence and presence of DOM (Figure 3c), and literature spectra of $FeOH^{2+}$ and $Fe(OH)_2^+$ species (Stefánsson, 2007). Ligand-to-metal charge transfer transitions have been attributed to iron(III) absorption spectra (Stefánsson, 2007, and references therein). The reported ε_{254} (6.53×10^{-2} L mg^{-1} cm^{-1}) is slightly lower than those observed by Weishaar et al. (2003) ($8.0\text{-}8.5 \times 10^{-2}$ L mg^{-1} cm^{-1}), which may be explained by the higher iron(III) concentrations used in their study. Despite this disparity, the quantifiable level of iron(III) for UV-vis interference in this study at λ = 254 nm (0.03 mg L^{-1}) adequately agrees with those previously reported (Weishaar et al., 2003). Although the iron(III) ε_{280} is smaller than ε_{254} (Table 2), $SUVA_{280}$ values for all DOM samples were more prone than $SUVA_{254}$ to iron(III) interference. Therefore, under most scenarios, lower UV wavelengths are preferred for DOM characterization due to prominent DOM absorption in this region regardless of greater absorption by iron(III).

It is important to recognize that iron(III) extinction coefficients were established in oxygen-free, iron(III)-DOM equilibrated systems. Iron commonly enters surface waters as iron(II) from numerous environmental processes (e.g., annual lake turnover (Maloney et al., 2005), diurnal photo-reduction (McKnight et al., 1988), and subsurface hydrologic pathways) and is subsequently oxidized to iron(III). Additionally, unless precautions are taken, iron(II) oxidation to iron(III) is likely in environmental samples collected for laboratory analysis. This suggests that iron(III) interference in environmental samples may differ from those observed in laboratory addition studies. Experiments conducted between pH 2 – 6.7 with added iron(II), where significant iron(II) oxidation was observed (Figure 1), provide insight on potential differences in UV-vis interference. Iron(III) generated from iron(II) oxidation showed less pronounced absorption maxima and broader absorption spectra (Figure 3d) than that of added iron(III) (Figure 3c). A combination of colloidal iron(III) (hydr)oxides (Sherman and Waite, 1985) and dissolved iron(III) species (Stefánsson, 2007) were likely responsible for this observation. Despite differences in

UV-vis absorption spectra, Suwannee River HPoA a_{254} values corrected for quantified iron(III) using ε_{254} were in good agreement with those of control samples (Figure 4). Iron(III)-corrected $SUVA_{254}$ values for these samples were within 5.3% of control samples across a range of iron(III) concentrations and pH values. This observation confirms that reported extinction coefficients are suitable for iron(III) correction of environmental samples. DOM absorption coefficients should be corrected using the reported iron(III) extinction coefficients prior to determination of optical parameters.

Empirically correcting DOM absorption coefficients for iron(III) offers several advantages over the chemical reduction method published by Doane and Horwáth (2010). Foremost, the reduction method relies on (1) pH adjustment for reductant efficiency and (2) UV-vis spectra correction for the reductant. Additionally, this method was only verified on iron(III)-DOM samples where iron(III) was equilibrated with DOM only "minutes" prior to reductant addition, and no tests confirmed effective iron(III) reduction when generated from iron(II) oxidation. Furthermore, potential irreversible transformations to DOM chemical properties upon chemical reduction (Maurer et al., 2010) could influence parallel DOM fluorescence measurements. Here, extinction coefficients were established with iron(III)-DOM equilibrated samples and validated for iron(III) formed from iron(II) oxidation. Empirical iron(III) correction does not require additional laboratory procedures and can be used to correct previously acquired data. Because iron(III) concentrations can easily and affordably be quantified using spectrophotometers in both lab and field settings, extinction coefficients offers a pragmatic solution to correct for iron(III).

Optical parameters based on relative (e.g., S_R, E_2:E_3), as opposed to absolute (e.g., $SUVA_{254}$), absorption proved more robust to iron(III) interference. For example, decreases in Everglades F1 water S_R and E_2:E_3 did not exceed 30% and 20% at 1.41 mg L^{-1} added iron(III), while $SUVA_{254}$ increased by 56%. In the latter case, the increase in measured $SUVA_{254}$ from 3.45 to 5.32 L mg_C^{-1} m^{-1} is effectively

equivalent to an increase in aromatic carbon content from 25.8 to 39.0% (Weishaar et al., 2003). It should be noted that isolated humic acid samples are known to have aromatic carbon contents of about 40% (Weishaar et al., 2003), yet these values are outside the range common of natural surface water samples ($SUVA_{254}$ < 5.0 L mg_C^{-1} m^{-1}) (Spencer et al., 2012). Similarly, measured S_R and E_2:E_3 values in the presence of iron(III) inferred DOM of greater bulk molecular weight (Helms et al., 2008) and relative size (De Haan and De Boer, 1987) (Figure A-5). Our finding that iron(III) reduces spectral slopes is consistent with two previous studies (Maloney et al., 2005; Pullin et al., 2007). Although both studies report spectral slopes over different wavelength intervals, trends showing a reduction in spectral slopes with increasing iron(III) (Pullin et al., 2007) or total iron (Maloney et al., 2005) are consistent with the reduction in $S_{275\text{-}295}$ observed in the present study. More pronounced decreases in S_R and E_2:E_3 ratios observed in Williams Lake water samples (Figure A-5) illustrates that water samples containing less prominent UV absorbing, aliphatic DOM are more susceptible to interference by iron(III).

Equally important was the observation that 0.03 mg L^{-1} iron(III), equivalent to the instrumental background absorption coefficient at 254 nm (Table 2), resulted in relatively minor increases (< 4%) in $SUVA_{254}$ of all DOM isolate and surface water samples. Therefore, quantifiable levels of iron(III) interference may not necessarily translate into substantial changes in optical parameters. Values in Table A-2 provide practitioners with iron(III) thresholds, equivalent to 5% of sample absorption coefficients, for UV-vis absorption measurements. Iron(III) thresholds at λ = 254 and 280 nm were always at environmental relevant concentrations (< 1 mg L^{-1}) even at high sample absorption coefficients (i.e., 1.0 cm^{-1}) which emphasize the importance of these results. Further discussion on UV-vis iron(III) effects can be found in the Appendix.

EFFECTS OF IRON ON DOM FLUORESCENCE

Despite increased Rayleigh scattering in iron(III)-containing samples (Figure A-3, A-4), the observed fluorescence reduction is attributed to ground-state iron-DOM interactions. Iron-quenching was observed regardless of oxidation state at pH 6.7 (Figure 5), while increased Rayleigh scattering was only observed upon iron(III) addition (Figure A-3). Quenching by iron was eliminated at pH ≤ 3 (Figure 8) likely due to proton competition for DOM functional groups (e.g., carboxylic acid). In addition, colloidal iron(III) formed through iron(II) oxidation at pH > 6 did not quench Suwannee River HPoA fluorescence (Figure 8), which has been previously reported (Waite and Morel, 1984; Cabaniss, 1992). These observations lend support to the conclusion that fluorescence reduction was due to static quenching (Waite and Morel, 1984; Senesi, 1990; Cabaniss, 1992; Ohno et al., 2007; Pullin et al., 2007) rather than a shift in DOM molecular weight distribution (Pullin et al., 2007) or inner filter effects from iron colloids (Lakowicz, 2006). The small levels of fluorescence enhancement of Williams Lake water at high iron(III):DOC is likely a result of increased light scattering from colloidal iron (Cabaniss, 1992; Lakowicz, 2006).

Numerous observations of iron(III) quenching of isolated riverine DOM (Waite and Morel, 1984; Senesi, 1990; Cabaniss, 1992; Pullin et al., 2007) and water-soluble soil organic matter (Ohno et al., 2007) have been made, but this is first published finding of comparable fluorescence quenching by iron(II). In oxic experimental conditions, there is both indirect (Pullin and Cabaniss, 2003) and direct (Gaffney et al., 2008; Jackson et al., 2012) evidence of iron(II)-DOM complexation controlling iron(II) oxidation rates (Pullin and Cabaniss, 2003; Gaffney et al., 2008). Similar interactions are likely responsible for observed iron(II) quenching in this study. However, Jackson et al. (2012) recently proposed the formation of weak iron(II)-DOM interactions under anoxic conditions, but strong iron(II)-DOM complexes formed under oxic conditions through dark thermal iron(III) reduction by DOM and subsequent iron(II)-DOM complex formation. It is unclear if iron redox cycling, as evidenced by low

levels of iron(II) oxidation (< 10%) in oxygen-free systems, resulted in stable iron(II)-DOM complex formation over the 24 h equilibration time, or if weak iron(II)-DOM interactions were responsible for quenching. Alternatively, iron(II) quenching through dynamic (i.e., collisional) interactions has not been observed with model fluorophores (Waite and Morel, 1984; Cha and Park, 1998) and, thus, is unlikely (further discussion can be found in the Appendix).

DOM compositional differences are attributed to contrasting iron-quenching behaviors observed between DOM samples. Iron complexation by higher-molecular weight, hydrophobic DOM is likely responsible for quenching observed in humic C and A peak regions (Wu et al., 2003) of HPoA samples (Figure 6, A-6, A-7). Similar iron(III) quenching behavior was observed with soil organic matter leachates (Ohno et al., 2007). Iron-quenching was never observed at short excitation/emission wavelengths attributed to low molecular weight phenols (Maie et al., 2007) and/or protein-like fluorophores (Coble, 1996), even in Williams Lake water which has autochthonous fluorescence signatures (Figure A-2). Equally notable were markedly different trends in degree and location of iron-quenching observed between Everglades F1 HPoA and Everglades F1 water samples (Figure 6, A-6, A-7). Greater overall iron-quenching of Everglades F1 water (Figure 5) suggests that certain fluorophores exhibit varying sensitivity to iron aside from properties of aromaticity or molecular weight. These differences were not explained by higher calcium concentrations in Everglades F1 water (Fu et al., 2007) or background trace metal levels observed to concentrate from DOM isolation (Table A-1) (Cabaniss, 1992; Zhao and Nelson, 2005; Pullin et al., 2007). A possible explanation is that greater carboxyl functional group content predicted of low aromatic DOM (e.g. filtered whole water) in comparison to the HPoA fraction (Aiken, 1985) would increase iron binding capacity, which would agree with observations by two previous studies (Ohno et al., 2007; Pullin et al., 2007).

Fluorescence indices proved susceptible to interferences due to iron quenching and pH effects. HPoA samples exhibited the greatest increase in FI values from iron due to preferential quenching at high excitation/emission wavelengths (Figure A-6, A-7) resulting in the suppression of the excitation 370 nm fluorescence peak (Figure 7). Iron effects on FI values were most severe (ΔFI = 0.13 FI units) at pH 4 (Figure A-9), which was likely due to simultaneous pH effects on fluorescence at long excitation/emission wavelengths (Figure 9). All of the abovementioned shifts in measured FI values inferred DOM source materials of greater autochthonous origin (McKnight et al., 2001). Because greater FI values were observed upon iron(II) and iron(III) additions at pH 6.7, these results are not attributed to the flocculation of hydrophobic DOM, which has been reported in the presence of aluminum sulfate coagulants (Beggs et al., 2009). However, Suwannee River HPoA exhibited elevated FI values in the presence of iron(III) formed from iron(II) oxidation (Figure A-9) even when the overall fluorescence was not quenched (Figure 8). The sorption of hydrophobic DOM to suspended iron colloids (Meier et al., 1999) may be responsible for this observations. Pullin and Cabaniss (2003) concluded that the initial iron oxidation state affects the amount of colloidal iron formed in the presence of DOM, with iron(II) yielding more colloidal iron in comparison to iron(III). This may explain why iron(III) generated from iron(II) oxidation did not quench DOM fluorescence, whereas added iron(III) did result in quenching (Figure 5). FI values determined at emission wavelengths of 450 and 500 nm were less susceptible to iron and pH effects than those at 470 and 520 nm (Figure A-9). Therefore, emission wavelengths of 450 and 500 nm are recommended for FI determination when used to infer DOM source material (further discussion in the Appendix) (McKnight et al., 2001). Iron levels, and those of other metals known to influence fluorescence (e.g., manganese, aluminum) (Cabaniss, 1992; Luster et al., 1996; Ohno et al., 2007), should be monitored and reported when conclusions are drawn on changes in FI values ≤ 0.15 FI units. FI values of iron-containing acidified samples (pH 2) were consistent with those of control samples, which

verify the acidification protocol put forth by McKnight et al. (2001) to minimize metal effects on fluorescence indices.

Equally important was the observed non-uniform fluorescence reduction of Suwannee River HPoA EEMs in the absence of iron between pH 6.7 – 2 (Figure 9). Locations of fluorescence reduction at pH 4 (~385/475 nm) is likely due to protonation of carboxyl functional groups of highly conjugated molecules (Figure 9e). The location of reduced fluorescence at pH 3 (~305/425 nm) (Figure 9f) closely match excitation/emission peaks of hydroxyl- and methoxy-substituted cinnamic and benzoic acids (Wolfbeis, 1985), which are known to be important structural moieties contributing to DOM fluorescence (Senesi, 1990). Surprisingly, the greatest reduction in fluorescence upon acidification was between pH 3 and 2 (Figure 8, 9g). The majority of DOM carboxyl functional groups are protonated at pH 3 (Aiken, 1985). One possible explanation for fluorescence reduction between pH 3 and 2 (Figure 9f, 9g) is the protonation of excited state phenols at pH < 3, which are known to be strong acids in the excited state (Wolfbeis et al., 1986). Common phenols moieties in DOM show significant overlap in fluorescence peak locations (Senesi, 1990), which would explain the ubiquitous fluorescence reduction observed at pH 2 (Figure 9g). The observation of non-uniform reduction in DOM fluorescence with acidification is corroborated by other studies (Senesi, 1990; Mobed et al., 1996; Spencer et al., 2007). These findings warrant concern over the use of acidification for sample preservation or as a means to eliminate metal associations prior to EEMs analysis (McKnight et al., 2001; Mladenov et al., 2010).

The deviation in PARAFAC modeling results observed upon acidification were proportional, or greater (Table A-3), than those observed at the highest iron:DOC. Using the 7-component model, six of the seven components differed by 2 – 6% at pH 5 when compared to pH 6.7 (Table A-3). Iron affects on PARAFAC component distributions were relatively small, or negligible, largely owing to the overlap between multiple PARAFAC components and iron-quenching locations. When quenching was observed

in precise regions at low iron levels (Figure 6, A-9, A-10), the degree of quenching was not substantial enough to significantly alter PARAFAC component distributions. Deviation in the 13-component modeling results at pH 6.7 were consistent between iron(II) and iron(III) titrations of HPoA samples, which suggests that static quenching was responsible for the reduction of C4 rather than the oxidation of hydroquinone moieties proposed to comprise this component (Cory and McKnight, 2005). Although component 7 of both models (denoted SQ2 in the 13-component model) share distinctly similar excitation/emission maxima (Cawley et al., 2012), changes in component distributions due to iron were only noted in the 7-component model. This observation, along with those of variable PARAFAC responses to pH (Table A-3), highlights an important pitfall of PARAFAC modeling. PARAFAC component distributions are based on the relative, as opposed to absolute, fluorescence intensity. Therefore, unless additional compound-specific analyses are performed, it should not be assumed that an increase in one component's contribution to the total fluorescence means there is "more" of this component.

This work also draws attention to the clear lack of accuracy, and sensitivity, in the use of fluorescence-quenching methods to derive metal-DOM stability constants (Ryan and Weber, 1982; Luster et al., 1996; Plaza et al., 2006; Ohno et al., 2007; Yamashita and Jaffé, 2008). Chief among these faults is that fluorescence quenching methods only investigate metal-fluorescent ligand interactions, and therefore do not account for complexation with non-fluorescent DOM molecules. The fraction of molecules in a DOM samples responsible for observed fluorescence is unknown, but will vary based on DOM compositional differences. Furthermore, DOM optical properties are understood to result from a combination of independent chromophores and a continuum of coupled excited states through intra-molecular charge-transfer interactions (Del Vecchio and Blough, 2004), which provides evidence that modeling a single binding site with fluorescence signals (Luster et al., 1996; Plaza et al., 2006) or PARAFAC components (Ohno et al., 2007; Yamashita and Jaffé, 2008) is inaccurate. Regarding the sensitivity of fluorescence-quenching methods, this study observed similar quenching strength by iron

regardless of oxidation for each DOM sample (Figure 5), which would not be predicted based on the hierarchy of iron-DOM binding strength (iron(III) > iron(II)) observed under anoxic conditions (Gaffney et al., 2008; Jackson et al., 2012). This lack of sensitivity is most evident in reported metal-DOM stability constants established for trace metals. For example, Yamashita and Jaffé (2008) report mercury(II)-DOM stability constants using fluorescence-quenching methods ~6-18 orders of magnitude lower than those previously established (Haitzer et al., 2002). Metal-DOM stability constants reported using fluorescence quenching methods should not be used in chemical speciation or aquatic toxicity models (e.g., biotic ligand model).

CONCLUSIONS AND IMPLICATIONS

The goal of this study was to resolve the influences of iron on pragmatic optical measurements used for DOM characterization in laboratory and *in situ* applications. Water systems most susceptible to UV-vis iron(III) interferences are those exhibiting diel (McKnight et al., 1988) or seasonal (Cory and McKnight, 2005; Maloney et al., 2005) fluctuations in iron concentration and/or oxidation state. Based exclusively on optical density, water samples with low DOC levels and/or DOM of low molar absorptivity are more prone to iron(III) interference. However, waters with elevated DOC levels and/or DOM of high molar absorptivity exhibit greater ability to slow rates of iron(III) hydrolysis and stabilize colloidal iron (Gaffney et al., 2008; Pédrot et al., 2011), and thus are also suspect to iron(III) interference. DOM characterization at shorter UV-vis wavelengths, and with spectral slope and absorption ratio parameters, are more robust to iron(III) affects. Iron(III) extinction coefficients provide a reasonable correction method for UV-vis absorption measurements. Not correcting for iron(III) absorbance will result in erroneous DOM UV-vis measurements, in example reported $SUVA_{254}$ values exceeding 5.0 L mg_C^{-1} m^{-1}, that do not reflect DOM properties.

Fluorescence interferences by iron(II) and iron(III) varied in significance between DOM source materials and with pH. Environmental samples at mildly acidic pH (4 – 5.5) are most prone to iron interferences due to slower rates of iron hydrolysis, limited proton competition for DOM functional groups, and coincident pH effects on DOM fluorescence. The variable fluorescence responses of different DOM samples draws attentions to the complexities of static quenching across a heterogeneous mix of natural fluorophores. For this reason, predicting fluorescence changes in environmental samples due to metals is unlikely. Acidification minimized iron quenching, but changes in DOM EEMs at low pH were evident and should not be ignored. PARAFAC modeling results were largely insensitive to interferences by iron, yet, this finding does not preclude the potential for metal interferences under all scenarios. The potential for fluorescence quenching and/or enhancement by other metals, principally manganese and aluminum (Cabaniss, 1992; Luster et al., 1996; Ohno et al., 2007), should be evaluated. The growing popularity of fluorescence spectroscopy as a pragmatic tool to monitor changes in DOM is apparent. However, the non-conservative behavior of DOM fluorescence illustrated in this study elucidates the inherent complexities of this method. A refined understanding of underlying chemical processes controlling DOM fluorescence will aid the application of these novel methods across environmental disciplines.

Iron affects on both UV-vis absorption and fluorescence measurements could have implications on the use of *in situ* fluorescence sensors in freshwater systems. *In situ* fluorescence probes measure the fluorescence fraction of chromophoric DOM (FDOM), and provide an inexpensive, high resolution proxy for DOC concentration and DOM quality (Downing et al., 2012). Iron could influence FDOM measurements in two ways. First, both dissolved and colloidal iron(III) could attenuate excitation and emission signals through absorbance and light scattering. Secondly, quenching by both iron(II) and iron(III) could reduce DOM fluorescence emission. Although commercially available *in situ* probes differ in the excitation (350 – 370 nm ± 10 – 20 nm bandpass) and emission (430 – 460 nm ± 30 – 120 nm

bandpass) wavelength specifications (Downing et al., 2012), all fluorescence measurements are taken in EEM regions where iron-quenched was observed. However, it is unclear to what extent iron would influence FDOM measurements. Light attenuation by dissolved substances and suspended particles, other than iron, are recognized to affect FDOM values (Downing et al., 2012). It could be that large fluctuations in iron levels coincide with high-flow hydrologic events, in which case iron may not be the only constituent of concern. Iron should be concurrently measured on samples collected for routine laboratory analysis when calibrating and/or confirming field FDOM measurements.

REFERENCES

Aeschbacher, M., Graf, C., Schwarzenback, R. P., and Sander, M., 2012, Antioxidant properties of humic substances. *Environmental Science & Technology* **46**, 4916-4925.

Aiken, G. R., McKnight, D. M., Wershaw, R. L., and MacCarthy, P. (eds), 1985, *Humic substances in soil, sediment, and water: geochemistry, isolation, and characterization*, John Wiley & Sons, New York, 692 pp.

Aiken, G. R., McKnight, D. M., Thorn, K. A., and Thurman, E. M., 1992, Isolation of hydrophilic organic acids from water using nonionic macroporous resins. *Organic Geochemistry* **18**, 567-573.

Aiken, G. R., Hsu-Kim, H., and Ryan, J. N., 2011, Influence of dissolved organic matter on the environmental fate of metals, nanoparticles, and colloids. *Environmental Science & Technology* **45**, 3196-3201.

Batchelli, S., Muller, F. L. L., Chang, K. C., and Lee, C. L., 2010, Evidence for strong but dynamic iron−humic colloidal associations in humic-rich coastal waters. *Environmental Science & Technology* **44**, 8485-8490.

Beggs, K. M. H., Summers, S. R., and McKnight, D. M., 2009, Characterizing chlorine oxidation of dissolved organic matter and disinfection by-product formation with fluorescence spectroscopy and parallel factor analysis. *Journal of Geophysical Research G: Biogeosciences* **114**, G04001, doi:10.1029/2009JG001009.

Bertilsson, S. and Tranvik, L. J. 2000, Photochemical transformation of dissolved organic matter in lakes. *Limnology and Oceanography* **45**, 753-762.

Cabaniss, S. E., 1992, Synchronous fluorescence spectra of metal-fulvic acid complexes. *Environmental Science & Technology* **26**, 1133-1139.

Cawley, K. M., Butler, K. D., Aiken, G. R., Larsen, L. G., Huntington, T. G., and McKnight, D. M., 2012, Identifying fluorescent pulp mill effluent in the Gulf of Maine and its watershed. *Marine Pollution Bulletin* **64**, 1678-1687.

Cha, K. W. and Park, K. W., 1998, Determination of iron(III) with salicylic acid by the fluorescence quenching method. *Talanta* **46**, 1567-1571.

Chin, Y. P., Aiken, G. R., and O'Loughlin, E., 1994, Molecular weight, polydispersity, and spectroscopic properties of aquatic humic substances. *Environmental Science & Technology* **28**, 1853-1858.

Coble, P. G., 1996, Characterization of marine and terrestrial DOM in seawater using excitation-emission matrix spectroscopy. *Marine Chemistry* **51**, 325-346.

Cory, R. M., 2005, Redox and photochemical reactivity of dissolved organic matter in surface waters. Ph.D. Dissertation, University of Colorado, Boulder, CO, 252 pp.

Cory, R. M. and McKnight D. M., 2005, Fluorescence spectroscopy reveals ubiquitous presence of oxidized and reduced quinones in dissolved organic matter. *Environmental Science & Technology* **39**, 8142-8149.

De Haan, H. and De Boer, T., 1987, Applicability of light absorbance and fluorescence as measures of concentration and molecular size of dissolved organic carbon in humic Lake Tjeukemeer. *Water Research* **21**, 731-734.

Del Vecchio, R. and Blough, N. V., 2004, On the origin of the optical properties of humic substances. *Environmental Science & Technology* **38**, 3885-3891.

Doane, T. A. and Horwáth, W. R., 2010, Eliminating interference from iron(III) for ultraviolet absorbance measurements of dissolved organic matter. *Chemosphere* **78**, 1409-1415.

Downing, B. D., Pellerin, B. A., Bergamaschi, B. A., Saraceno, J. F., and Kraus, T. E. C., 2012, Seeing the light: The effects of particles, dissolved materials, and temperature on in situ measurements of DOM fluorescence in rivers and streams. *Limnology and Oceanography: Methods* **10**, 767-775.

Fu, P., Wu, F., Congqiang, L., Wang, F., Li., W., Yue, L., and Guo, Q., 2007, Fluorescence characterization of dissolved organic matter in an urban river and its complexation with Hg(II). *Applied Geochemistry* **22**, 1668-1679.

Gaffney, J. W., White, K. N., and Boult, S., 2008, Oxidation state and size of Fe controlled by organic matter in natural waters. *Environmental Science & Technology* **42**, 3575-3581.

Gustafsson, J. P., 2011, Visual MINTEQ version 3.0, Stockholm, Sweden.

Helms, J. R., Stubbins, A., Ritchie, J. D., and Minor, E. C., 2008, Absorption spectral slopes and slope ratios as indicators of molecular weight, source, and photobleaching of chromophoric dissolved organic matter. *Limnology and Oceanography* **53**, 955-969.

Jackson, A., Gaffney, J. W., and Boult, S. 2012, Subsurface interactions of Fe(II) with humic acid or landfill leachate do not control subsequent iron(III) (hydr)oxide production at the surface. *Environmental Science & Technology* **46**, 7543-7550.

Klapper, L., McKnight, D. M., Fulton, J. R., Blunt-Harris, E. L., Nevin, K. P., Lovley, D. R., and Hatcher, P. G., 2002, Fulvic acid oxidation state detection using fluorescence spectroscopy. *Environmental Science & Technology* **36**, 3170-3175.

Lakowicz, J. R., 2006, *Principles of Fluorescence Spectroscopy*, 3rd Edition, Springer Science+Business Media, New York, 954 pp.

Luster, J., Lloyd, T., and Sposito, G., 1996, Multi-wavelength molecular fluorescence spectrometry for quantitative characterization of copper(II) and aluminum(III) complexation by dissolved organic matter. *Environmental Science & Technology* **30**, 1565-1574.

Maie, N., Scully, N. M., Pisani, O., and Jaffé, R., 2007, Composition of a protein-like fluorophore of dissolved organic matter in coastal wetland and estuarine ecosystems. *Water Research* **41**, 563-570.

Maloney, K. O., Morris, D. P., Moses, C. O., and Osburn, C. L., 2005, The role of iron and dissolved organic carbon in the absorption of ultraviolet radiation in humic lake water. *Biogeochemistry* **75**, 393-407.

Maurer, F., Christl, I., and Kretzschmar, R., 2010, Reduction and reoxidation of humic acid: Influence on spectroscopic properties and proton binding. *Environmental Science & Technology* **44**, 5787-5792.

McKnight, D. M., Boyer, E. W., Westerhoff, P. K., Doran, P. T., Kulbe, T., and Andersen, D. T., 2001, Spectrofluorometric characterization of dissolved organic matter for indication of precursor organic material and aromaticity. *Limnology and Oceanography* **46**, 38-48.

McKnight, D. M., Kimball, B. A., and Bencala, K. E., 1988, Iron photoreduction and oxidation in an acidic mountain stream. *Science* **240**, 637-640.

Meier, M., Namjesnik-Dejanovic, K., Maurice, P. A., Chin, Y. P., and Aiken, G. R., 1999, Fractionation of aquatic natural organic matter upon sorption to goethite and kaolinite. *Chemical Geology* **157**, 275-284.

Mladenov, N., Zheng, Y., Miller, M. P., Nemergut, D. R., Legg, T., Simone, B., Hageman, C., Rahman, M. M., Ahmed, K. M., and McKnight, D. M., 2010, Dissolved organic matter sources and consequences for iron and arsenic mobilization in Bangladesh aquifers. *Environmental Science & Technology* **44**, 123-128.

Mobed, J. J., Hemmingsen, S. L., Autry, J. L., and McGown, L. B., 1996, Fluorescence characterization of IHSS humic substances: Total luminescence spectra with absorbance correction. *Environmental Science & Technology* **30**, 3061-3065.

Ohno, T., Amirbahman, A., and Bro, R., 2007, Parallel factor analysis of excitation–emission matrix fluorescence spectra of water soluble soil organic matter as basis for the determination of conditional metal binding parameters. *Environmental Science & Technology* **42**, 186-192.

Pédrot, M., Boudec, A. L., Davranche, M., Dia, A., and Henin, O., 2011, How does organic matter constrain the nature, size and availability of Fe nanoparticles for biological reduction? *Journal of Colloid and Interface Science* **359**, 11-11.

Plaza, C., Brunetti, G., Senesi, N., and Polo, A., 2006, Molecular and quantitative analysis of metal ion binding to humic acids from sewage sludge and sludge-amended soils by fluorescence spectroscopy. *Environmental Science & Technology* **40**, 917-923.

Provenzano, M. R., D'Orazio, V., Jerzykiewicz, M., and Senesi, N., 2004, Fluorescence behaviour of Zn and Ni complexes of humic acids from different sources. *Chemosphere* **55**, 885-892.

Pullin, M. J., Anthony, C., and Maurice, P. A., 2007, Effects of iron on the molecular weight distribution, light absorption, and fluorescence properties of natural organic matter. *Environmental Engineering Science* **24**, 987-997.

Pullin, M. J. and Cabaniss, S. E., 2003, The effects of pH, ionic strength, and iron-fulvic acid interactions on the kinetics of non-photochemical iron transformations. I. Iron(II) oxidation and iron(III) colloid formation. *Geochimica et Cosmochimica Acta* **67**, 4067-4077.

Pullin, M. J. and Cabaniss, S. E., 2003, The effects of pH, ionic strength, and iron-fulvic acid interactions on the kinetics of non-photochemical iron transformations. II. The kinetics of thermal reduction. *Geochimica et Cosmochimica Acta* **67**, 4079-4089.

Ryan, D. K. and Weber, J. H., 1982, Fluorescence quenching titration for determination of complexing capacities and stability constants of fulvic acid. *Analytical Chemistry* **54**, 986-990.

Senesi, N., 1990, Molecular and quantitative aspects of the chemistry of fulvic acid and its interactions with metal ions and organic chemicals: Part II. The fluorescence spectroscopy approach. *Analytica Chimica Acta* **232**, 77-106.

Sherman, D. M. and Waite, T. D., 1985, Electronic spectra of Fe^{3+} oxides and oxide hydroxides in the near IR to near UV. *American Mineralogist* **70**, 1262-1269.

Spencer, R. G. M., Bolton, L., and Baker, A., 2007, Freeze/thaw and pH effects on freshwater dissolved organic matter fluorescence and absorbance properties from a number of UK locations. *Water Research* **41**, 2941-2950.

Spencer, R. G. M., Butler, K. D., and Aiken, G. R., 2012, Dissolved organic carbon and chromophoric dissolved organic matter properties of rivers in the USA. *Journal of Geophysical Research G: Biogeosciences* **117**, G03001, doi:10.1029/2011JG001928.

Stedmon, C. A., Markager, S., and Bro, R., 2003, Tracing dissolved organic matter in aquatic environments using a new approach to fluorescence spectroscopy. *Marine Chemistry* **82**, 239-254.

Stefánsson, A., 2007, Iron(III) hydrolysis and solubility at 25 °C. *Environmental Science & Technology* **41**, 6117-6123.

Stumm, W., and Morgan, J. J., 1996, Aquatic chemistry: chemical equilibria and rates in natural waters, 3rd Edition, John Wiley & Sons, New York, 1022 pp.

To, T. B., Nordstrom, D. K., Cunningham, K. M., Ball, J. W., and McCleskey, R. B., 1999, New method for the direct determination of dissolved Fe(III) concentration in acid mine waters. *Environmental Science & Technology* **33**, 807-813.

Waite, T. D. and Morel, F. M. M., 1984, Ligand exchange and fluorescence quenching studies of the fulvic acid-iron interaction: Effects of pH and light. *Analytica Chimica Acta* **162**, 263-274.

Weishaar, J. L., Aiken, G. R., Bergamaschi, B. A., Fram, M. S., Fujii, R., and Mopper, K., 2003, Evaluation of specific ultraviolet absorbance as an indicator of the chemical composition and reactivity of dissolved organic carbon. *Environmental Science & Technology* **37**, 4702-4708.

Wolfbeis, O. S. (Schulman, S. G., ed), 1985, *The fluorescence of organic natural products, In Molecular Luminescence Spectroscopy - Methods and Applications; Part 1*, John Wiley and Sons, New York, 167-370 pp.

Wolfbeis, O. S., Begum, M., and Hochmuth, P., 1986, An unusual excited state species of ortho- hydroxy-cinnamic acid. *Photochemistry and Photobiology* **44**, 551-554.

Wu, F. C., Evans, R. D., and Dillon, P. J., 2003, Separation and characterization of NOM by high-performance liquid chromatography and on-line three-dimensional excitation emission matrix fluorescence detection. *Environmental Science & Technology* **37**, 3687-3693.

Yamashita, Y. and Jaffé, R., 2008, Characterizing the interactions between trace metals and dissolved organic matter using excitation-emission matrix and parallel factor analysis. *Environmental Science and Technology* **42**, 7374-7379.

Zhao, J. and Nelson, D. J., 2005, Fluorescence study of the interaction of Suwannee River fulvic acid with metal ions and Al^{3+}-metal ion competition. *Journal of Inorganic Biochemistry* **99**, 383-396.

APPENDIX

ION AND METAL CONCENTRATIONS OF EXPERIMENTAL SOLUTIONS

Surface water samples and DOM isolates were measured for other metals – namely Al, Cu, and Co – to insure that sample did not contain significant levels of metals known to quench or enhance DOM fluorescence. Concentrations of metals were well below levels reported to induce changes in DOM fluorescence properties (Senesi, 1990; Cabaniss, 1992; Plaza et al., 2006). Although metal concentrations for Williams Lake water were not available due to a lost sample, historic (1980 – 2010) metal concentrations of Williams Lake surface waters from the United States Geological Survey (USGS) Shingobee Headwaters Aquatic Ecosystems Program (SHAEP) did not show appreciable levels of Mn (< 0.002 mg L^{-1}), Cu (< 0.03 µg L^{-1}), Ni (< 0.04 µg L^{-1}), or Zn (< 0.03 µg L^{-1}).

Table A- 1. Ion and metal concentrations of surface water samples and DOM isolates of experimental solutions.

	Suwannee River HPoA (GA)	Everglades F1 HPoA (FL)	Everglades F1 water (FL)	Williams Lake water (MN)
Cl^- (mg L^{-1})	< 0.02	< 0.02	25.0	1.8
NO_3^- (mg L^{-1})	0.11	< 0.05	< 0.01	1.3
SO_4^{2-} (mg L^{-1})	< 0.2	< 0.2	4.2	1.3
NH_4^+ (mg L^{-1})	NA	NA	< 0.02	1.8
Na^+ (mg L^{-1})	1.02	1.21	22.1	< 0.02
K^+ (mg L^{-1})	< 0.10	< 0.10	0.8	0.5
Mg^{2+} (mg L^{-1})	< 0.02	< 0.02	2.4	5.1
Ca^{2+} (mg L^{-1})	0.09	0.12	7.9	14.6
Fe (mg L^{-1})	< 0.01	< 0.01	< 0.01	< 0.01
Mn (mg L^{-1})	< 0.002	<0.002	0.003	N/A
Co (µg L^{-1})	< 0.04	<0.02	< 0.04	N/A
Cu (µg L^{-1})	2.0	<1.12	6.7	N/A
Ni (µg L^{-1})	0.3	<0.26	0.4	N/A
Zn (µg L^{-1})	< 1.69	<0.43	< 1.69	N/A

Ions determined by ion chromatography; trace and major metal concentrations determined by acidification (1% HNO_3) and measured by inductively coupled plasma mass spectrometry (ICP-MS) and inductively coupled plasma optical emission spectrometry (ICP-OES); N/A, not available.

IRON(III) CONCENTRATION THRESHOLDS FOR UV-VIS ABSORPTION MEASUREMENTS

Table A- 2. Iron(III) concentration thresholds that represent a significant source (5%) of spectroscopic interference at 254, 280 and 400 nm wavelengths for sample absorption coefficients (a_λ) between 0.10 – 1.0 cm^{-1}. Thresholds do not predict how iron(III) will translate to uncertainties in optical parameters.

a_{254} (cm^{-1})	[iron(III)] ($mg\ L^{-1}$)	a_{280} (cm^{-1})	[iron(III)] ($mg\ L^{-1}$)	a_{400} (cm^{-1})	[iron(III)] ($mg\ L^{-1}$)
0.10	0.07	0.10	0.09	0.10	0.40
0.20	0.15	0.20	0.17	0.20	0.16
0.30	0.22	0.30	0.26	0.30	1.21
0.40	0.30	0.40	0.34	0.40	1.61
0.50	0.37	0.50	0.43	0.50	2.02
0.60	0.44	0.60	0.52	0.60	2.42
0.70	0.52	0.70	0.60	0.70	2.82
0.80	0.59	0.80	0.69	0.80	3.23
0.90	0.63	0.90	0.77	0.90	3.63
1.00	0.74	1.00	0.86	1.00	4.03

Table A- 3. PARAFAC model component distributions of Suwannee River HPoA in the presence and absence of iron; values are averages of experimental duplicates. Difference in component distributions between experimental duplicates did not exceed 0.7% and 1.3% in the 13- and 7-component models in all samples. pH 5.0 samples in the presence of iron omitted due to deviation from target pH.

	Control: Suwannee River HPoA (no iron)							Suwannee River HPoA + 0.68 mg L^{-1} iron					
13-Component Model[a]	**pH 6.7**	**pH 6**	**pH 5.5**	**pH 5**	**pH 4**	**pH 3**	**pH 2**	**pH 6.7**	**pH 6**	**pH 5.5**	**pH 4**	**pH 3**	**pH 2**
C1	12%	12%	13%	13%	13%	15%	14%	11%	12%	13%	15%	15%	14%
C2 (Q2)	17%	16%	16%	16%	15%	16%	16%	18%	17%	17%	16%	16%	16%
C3	1%	1%	1%	1%	1%	1%	2%	2%	1%	1%	1%	1%	2%
C4 (HQ)	26%	27%	27%	27%	26%	24%	24%	26%	25%	24%	23%	24%	24%
C5 (SQ1)	10%	10%	10%	10%	9%	9%	9%	9%	9%	8%	8%	9%	9%
C6	9%	10%	11%	11%	11%	10%	10%	7%	9%	10%	10%	10%	10%
C7 (SQ2)	5%	4%	3%	3%	2%	3%	2%	7%	5%	4%	4%	3%	2%
C8 (trp-like)	0%	0%	0%	0%	0%	0%	0%	0%	0%	0%	0%	0%	1%
C9 (SQ3)	0%	0%	0%	0%	0%	0%	0%	0%	0%	0%	0%	0%	0%
C10	6%	6%	6%	6%	5%	5%	4%	5%	6%	6%	6%	5%	4%
C11 (Q1)	8%	8%	8%	8%	8%	8%	8%	8%	8%	9%	9%	8%	8%
C12 (Q3)	4%	4%	4%	4%	4%	5%	6%	5%	5%	5%	5%	5%	6%
C13 (tyr-like)	2%	2%	2%	2%	3%	3%	3%	2%	3%	3%	3%	3%	4%
7-Component Model[b]	**pH 6.7**	**pH 6**	**pH 5.5**	**pH 5**	**pH 4**	**pH 3**	**pH 2**	**pH 6.7**	**pH 6**	**pH 5.5**	**pH 4**	**pH 3**	**pH 2**
C1	28%	29%	29%	30%	30%	31%	28%	25%	28%	28%	29%	27%	25%
C2	30%	32%	32%	35%	33%	34%	30%	27%	30%	23%	31%	30%	27%
C3	25%	24%	24%	19%	22%	22%	25%	28%	23%	23%	21%	21%	28%
C4	7%	7%	7%	8%	6%	6%	7%	8%	8%	8%	9%	9%	8%
C5	2%	2%	2%	4%	2%	2%	2%	2%	2%	2%	2%	2%	2%
C6	4%	5%	5%	2%	5%	5%	4%	4%	4%	4%	5%	5%	4%
C7	4%	2%	2%	2%	1%	1%	4%	7%	4%	4%	4%	5%	7%

[a](Cory and McKnight, 2005).
[b](Cawley et al., 2012).

IRON(III)-DOM EQUILIBRATION TIME

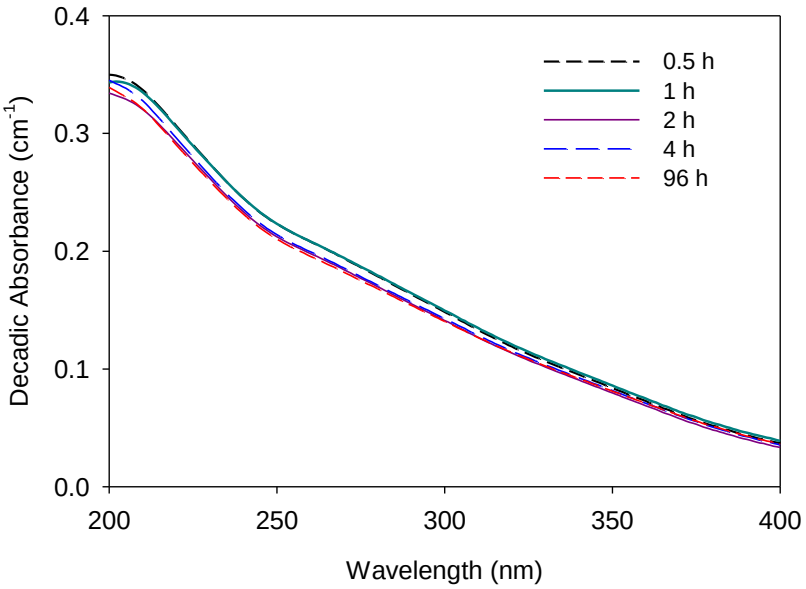

Figure A- 1. UV-vis absorption spectra of Suwannee River HPoA in the presence of 1.5 mg L^{-1} iron(III) equilibrated between 0.5 – 96 h.

EEMs OF DOM ISOLATES AND SURFACE WATER SAMPLES

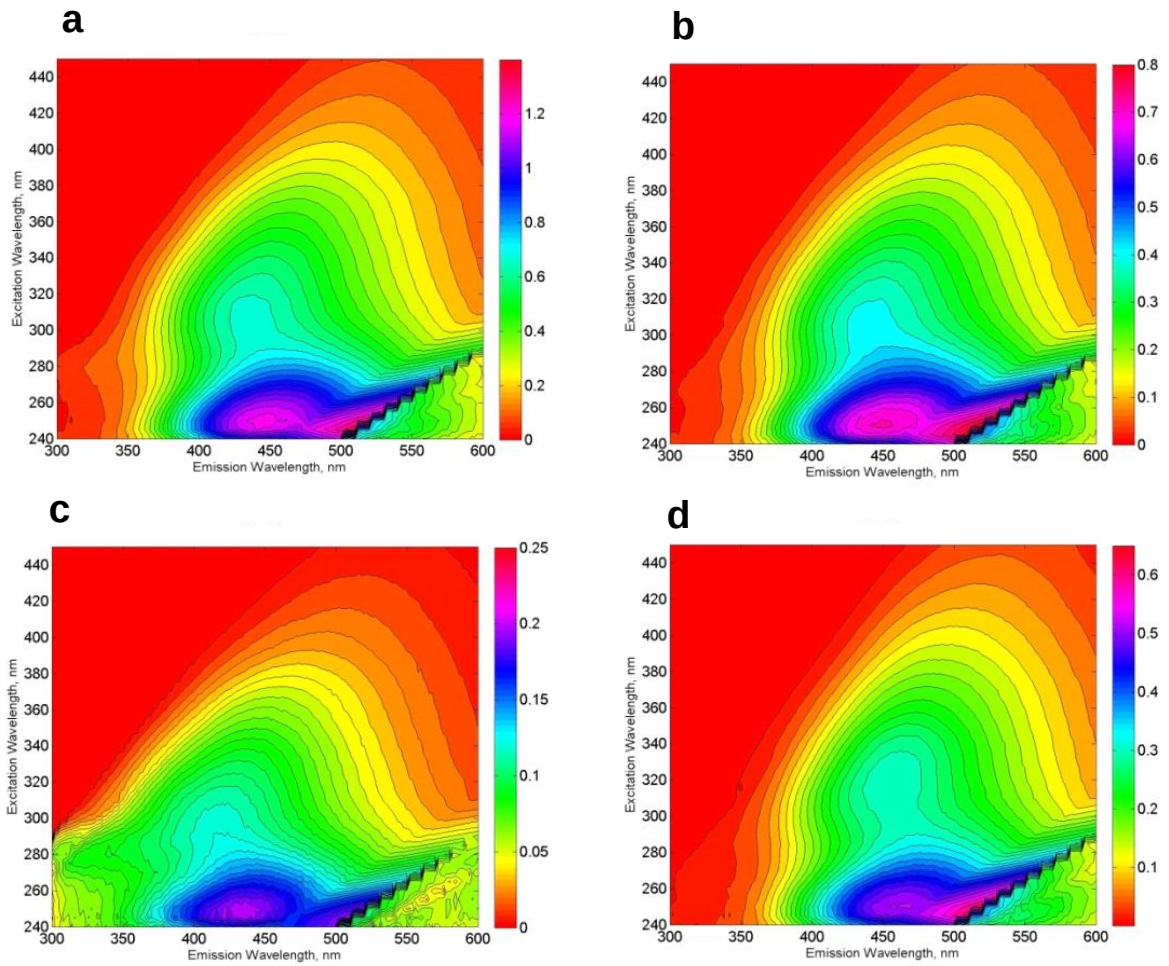

Figure A- 2. Excitation-emission matrices (EEMs) of (a) Everglades F1 water, (b) Everglades F1 HPoA, (c) Williams Lake water, and (d) Suwannee River HPoA at pH 6.7.

ESTIMATES OF DOM ELECTRON-DONATING CAPACITY

The electron-donating capacity of Suwannee River HPoA and Williams Lake water were estimated using recently published values for IHSS DOM isolates (Aeschbacher et al., 2012). The electron equivalents of observed levels of iron(III) reduction were then compared to estimates of DOM electron-donating capacity. The 2.49 $mg_C\ L^{-1}$ Suwannee River HPoA sample used in this study encompasses both humic and fulvic acid. The electron-donating capacities of 2.49 $mg_C\ L^{-1}$ Suwannee River humic (1.83 $mmol_{e^-}\ gDOM^{-1}$ at 43.3% carbon) and fulvic acid (1.37 $mmol_{e^-}\ gDOM^{-1}$ at 43.4% carbon) were estimated to be 1.06 and 0.79 μmol_{e^-} (pH 7, E_h 0.61 V) (Aeschbacher et al., 2012), respectively. Iron(III) reduction varied from 0.05 – 0.07 mg L^{-1} in Suwannee River HPoA systems depending on the titrated iron concentration, which is equivalent to 0.09 – 0.13 μmol_{e^-}. The estimated electron-donating capacities of Suwannee River humic and fulvic acid were always greater than eight fold and six fold that of the electrons equivalence of 0.07 mg L^{-1} iron(III) reduction, respectively. Pony Lake fulvic acid reference was used to estimates the electron-donating capacity of 4.50 $mg_C\ L^{-1}$ Williams Lake water due to both samples having lower molecular weight, autochthonous qualities. When assuming that Pony Lake fulvic acid comprised 100% of Williams Lake water DOC, the electron-donating capacity of 4.50 $mg_C\ L^{-1}$ Pony Lake fulvic acid (0.49 $mmol_{e^-}\ gDOM^{-1}$ at 43.2% carbon) was estimated to be 0.51 μmol_{e^-}. A maximum of 0.02 mg L^{-1} iron(III) reduction (0.036 μmol_{e^-}) was observed in the presence of Williams Lake water, which was less than fourteen fold the estimated electron-donating capacity. When assuming that 50% Williams Lake water DOC was composed of Pony Lake fulvic acid, the electron-donating capacity exceeded electron equivalence seven fold. Under these scenarios the electron-donating capacities of samples always well exceeded the electron equivalence of reduced iron(III). These analyses provide evidence that the oxidation of electron-donating moieties in DOM due to iron(III) reduction was likely insufficient to change DOM fluorescence properties.

RAYLEIGH SCATTERING OF FLUORESCENCE SPECTRA

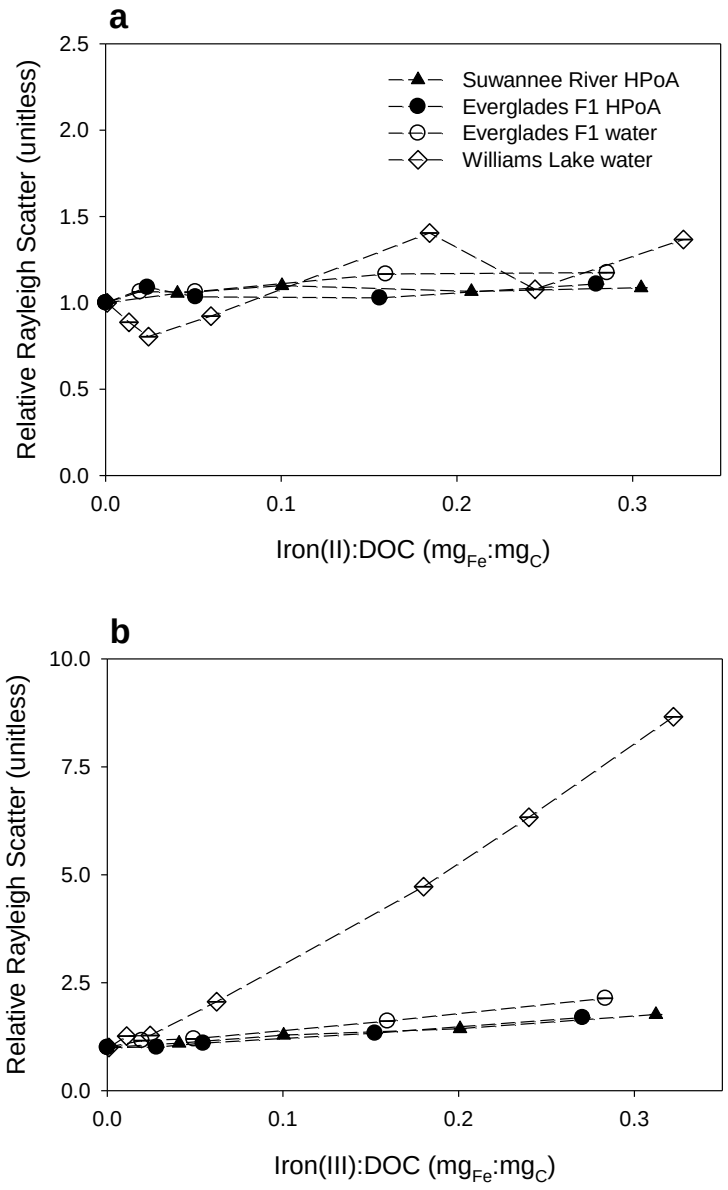

Figure A- 3. Relative changes in Rayleigh scatter measured at excitation/emission 350/350 nm in (a) iron(II) and (b) iron(III) titrations with increasing iron:DOC at pH 6.7. Data points are mean values of experimental duplicates with error bars indicating the high and low values observed.

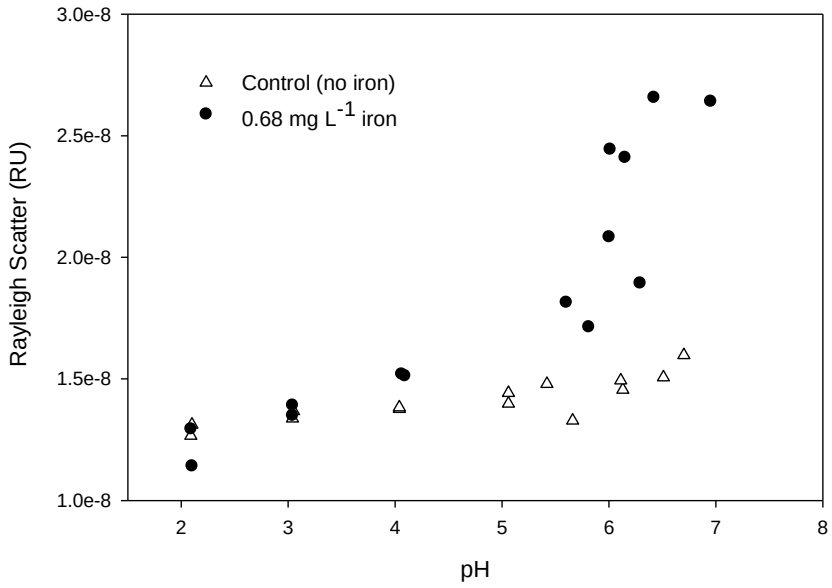

Figure A- 4. The Rayleigh scatter measured at excitation/emission 350/350 nm of solutions equilibrated for 24 h with 0.68 mg L^{-1} iron, added as iron(II), in the presence of 2.48 mg_C L^{-1} Suwannee River HPoA between pH 2 – 6.7. Data points are from single samples.

EFFECTS OF IRON(III) ON UV ABSORPTION COEFFICIENTS AND PARAMETERS

Results showing the additive effects of iron(III) on absorption coefficients are in agreement with iron(III) addition experiments conducted by Weishaar et al. (2003), and observations by Maloney et al. (2005) of a strong linear correlation between total iron concentrations of oxygenated lake waters and Naperian absorption coefficients at 320 nm. These findings contradict those detailed by Pullin et al. (2007), which conclude no significant increase in DOM absorption coefficients at 254 and 280 nm in the presence of iron(III), and more substantial contributions at wavelengths in the visible spectrum. It is possible that the lower iron(III):DOC used by Pullin et al. (2007) ($\leq 0.11\ mg_{Fe}:mg_{C}$) confounded their ability to resolve the influence of iron(III) due to the predominance of DOM absorption in this region.

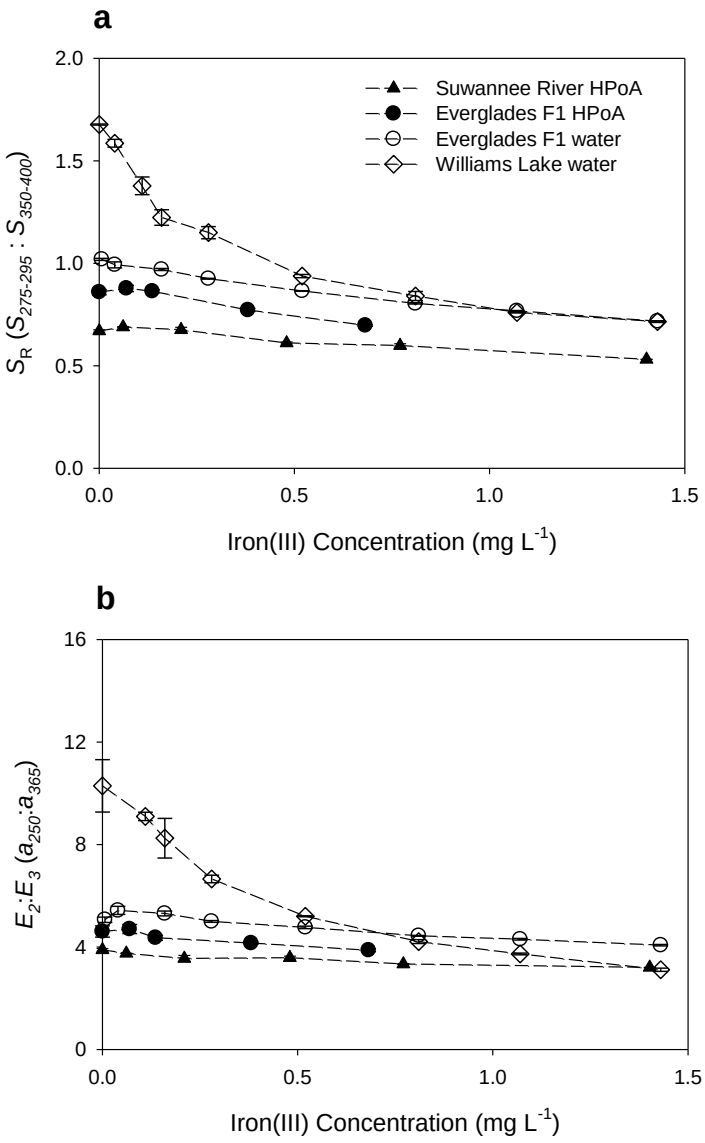

Figure A- 5. Increasing iron(III) concentration shows a negative relationship with (a) spectral slope ratio (S_R) and (b) E_2:E_3 ratio (a_{250}:a_{365}). Data points are mean values of experimental duplicates with error bars indicating the high and low values observed.

FLUORESCENCE QUENCHING BY IRON

Numerous studies have either confirmed or negated static fluorescence quenching of DOM by iron(II). First, Waite and Morel (1984) observed iron(II) to quenching Suwannee Rive fulvic acid (IHSS) by ~5% (excitation/emission 330/445 nm) at an iron(II):DOC of 0.22 mg_{Fe}:mg_C as a solution pH of 6.5. Slightly greater quenching efficiency was observed at pH 3.9 presumably due to slower rates of iron(II) oxidation and colloid formation at lower pH. Another study by Pullin et al. (2007) showed no significant iron(II) quenching. Though, because experiments by Pullin et al. (2007) employed a chemical reductant to prevent iron(II) oxidation, it is possible that increases in DOM fluorescence yield via DOM reduction (Klapper et al., 2002; Cory and McKnight, 2005) masked the coincident decrease in fluorescence due to iron(II) quenching. Lastly, another laboratory addition study observed fluorescence enhancement at low iron(II) levels (0.03 – 0.06 mg L^{-1}) and quenching at higher concentrations (0.28 – 2.79 mg L^{-1}) (Cory, 2005). However, it is unclear if iron(II) stock solutions prepared with oxidatively inert iron(II) salts (ferrous ethylene diammonium sulfate) may have resulted in the conflicting findings. One possibility is that the small levels of fluorescence enhancement at low iron(II) were a consequence of solution constituents reducing the DOM. Furthermore, the quenching observed at higher iron(II) levels may have been observed because the metal concentration was sufficiently high to quench fluorescence. In the present study, iron(II) oxidation was minimized by performing all experimental procedures under a 95% N_2/5% H_2 atmosphere and iron(II) stock solutions were prepared with $FeSO_4(H_2O)_7$, reaffirming our findings of fluorescence quenching by iron(II).

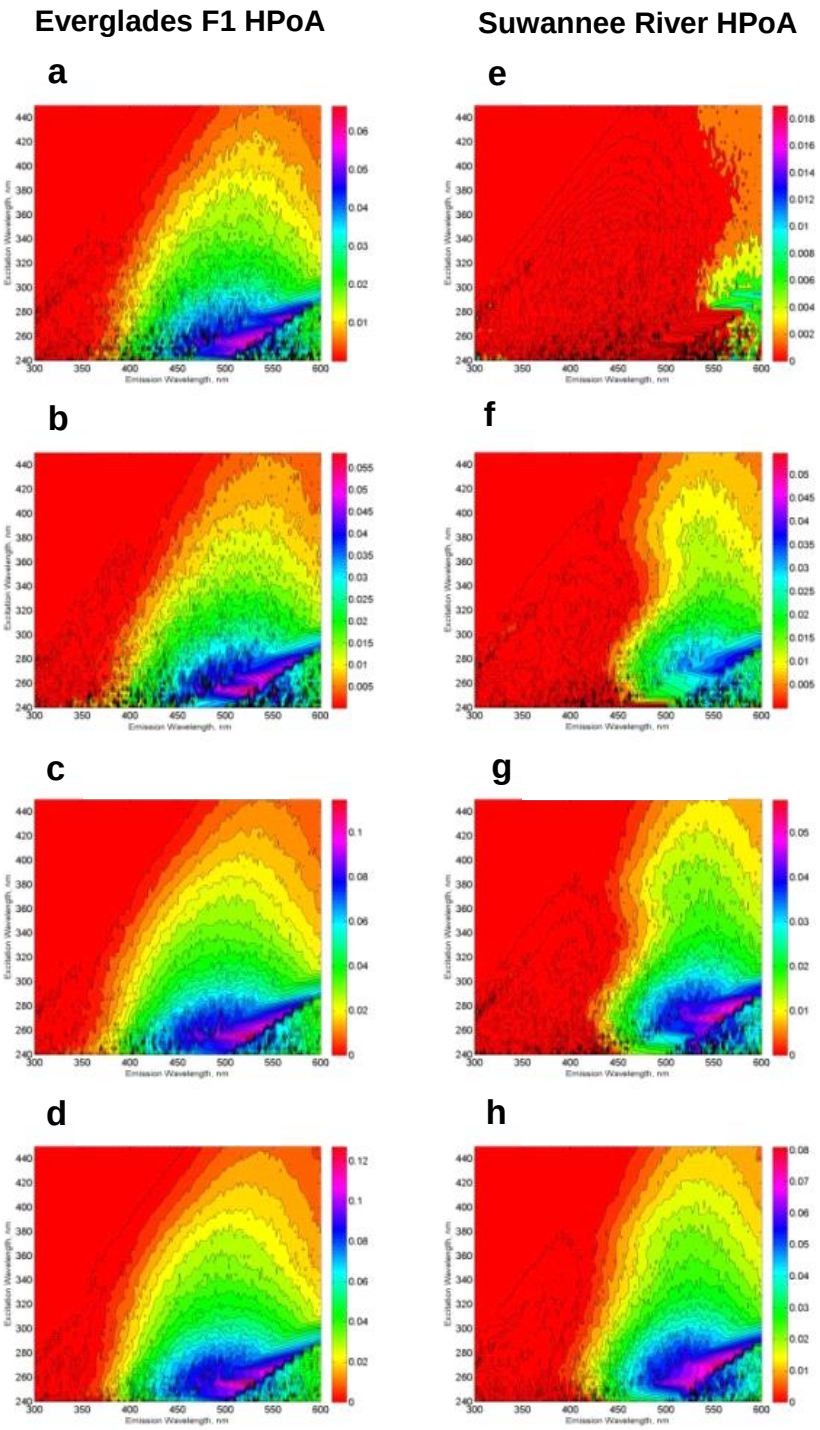

Figure A- 6. EEMs of fluorescence quenched (EEM_{FQ}) of Everglades F1 HPoA at iron(II):DOC = 0.02 (a), 0.05 (b), 0.16 (c) and 0.28 mg_{Fe}:mg_C (d) and Suwannee River HPoA at iron(II):DOC = 0.04 (e), 0.10 (f), 0.21 (g) and 0.31 mg_{Fe}:mg_C (h). All fluorescence intensities are in Raman units and EEM_{FQ} are not normalized to the same fluorescence intensity.

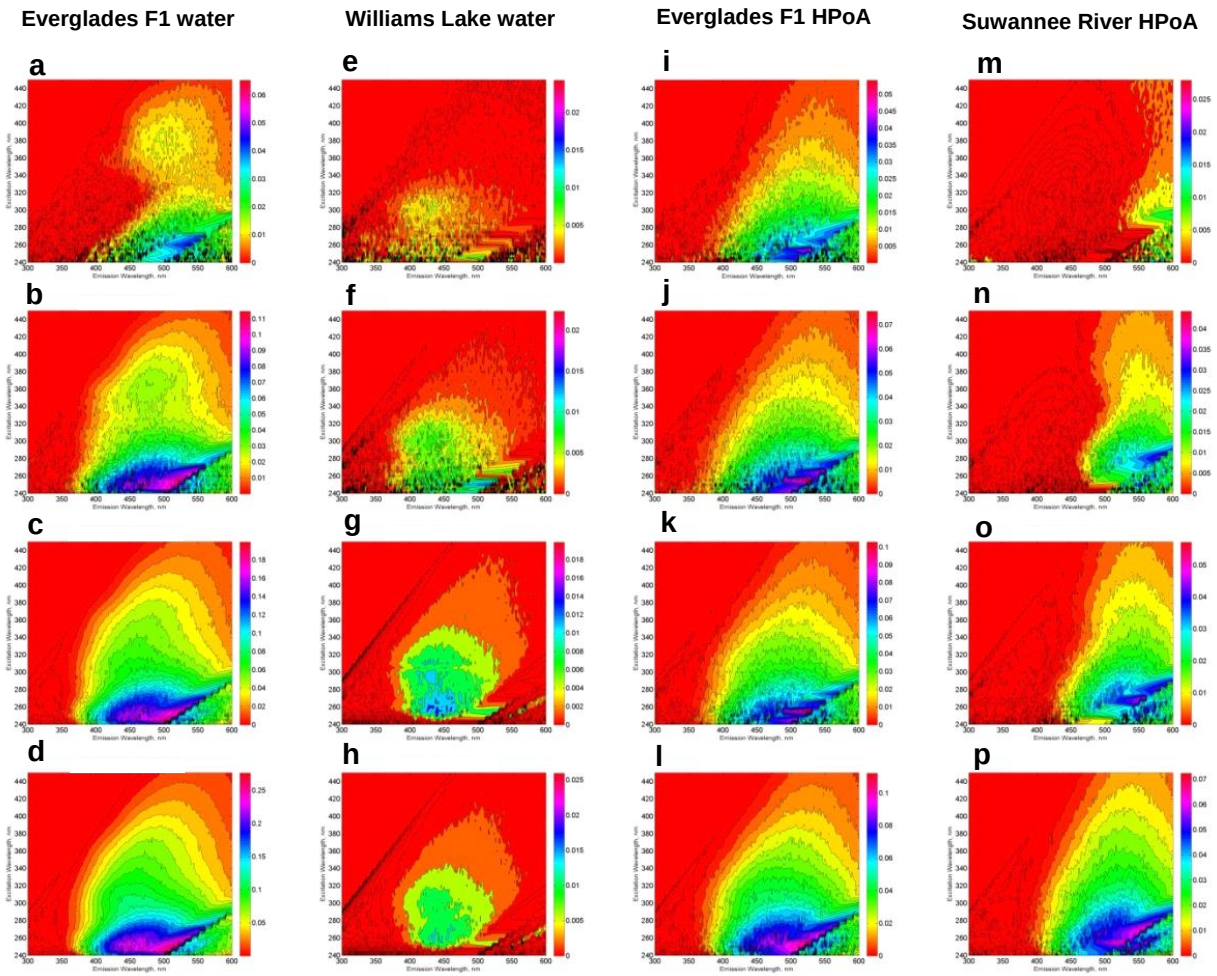

Figure A- 7. EEMs of fluorescence quenched (EEM_{FQ}) of Everglades F1 water at iron(III):DOC = 0.02 (a), 0.05 (b), 0.16 (c) and 0.28 mg_{Fe}:mg_C (d), Williams Lake water at iron(III):DOC = 0.02 (e), 0.06 (f), 0.18 (g) and 0.24 mg_{Fe}:mg_C (h), Everglades F1 HPoA at iron(III):DOC = 0.03 (i), 0.06 (j), 0.15 (k) 0.27 mg_{Fe}:mg_C (l), Suwannee River HPoA at iron(III):DOC = 0.04 (m), 0.10 (m), 0.20 (o) and 0.31 mg_{Fe}:mg_C (p). All fluorescence intensities are in Raman units and EEM_{FQ} are not normalized to the same fluorescence intensity.

pH EFFECTS ON DOM FLUORESCENCE IN THE PRESENCE AND ABSENCE OF IRON

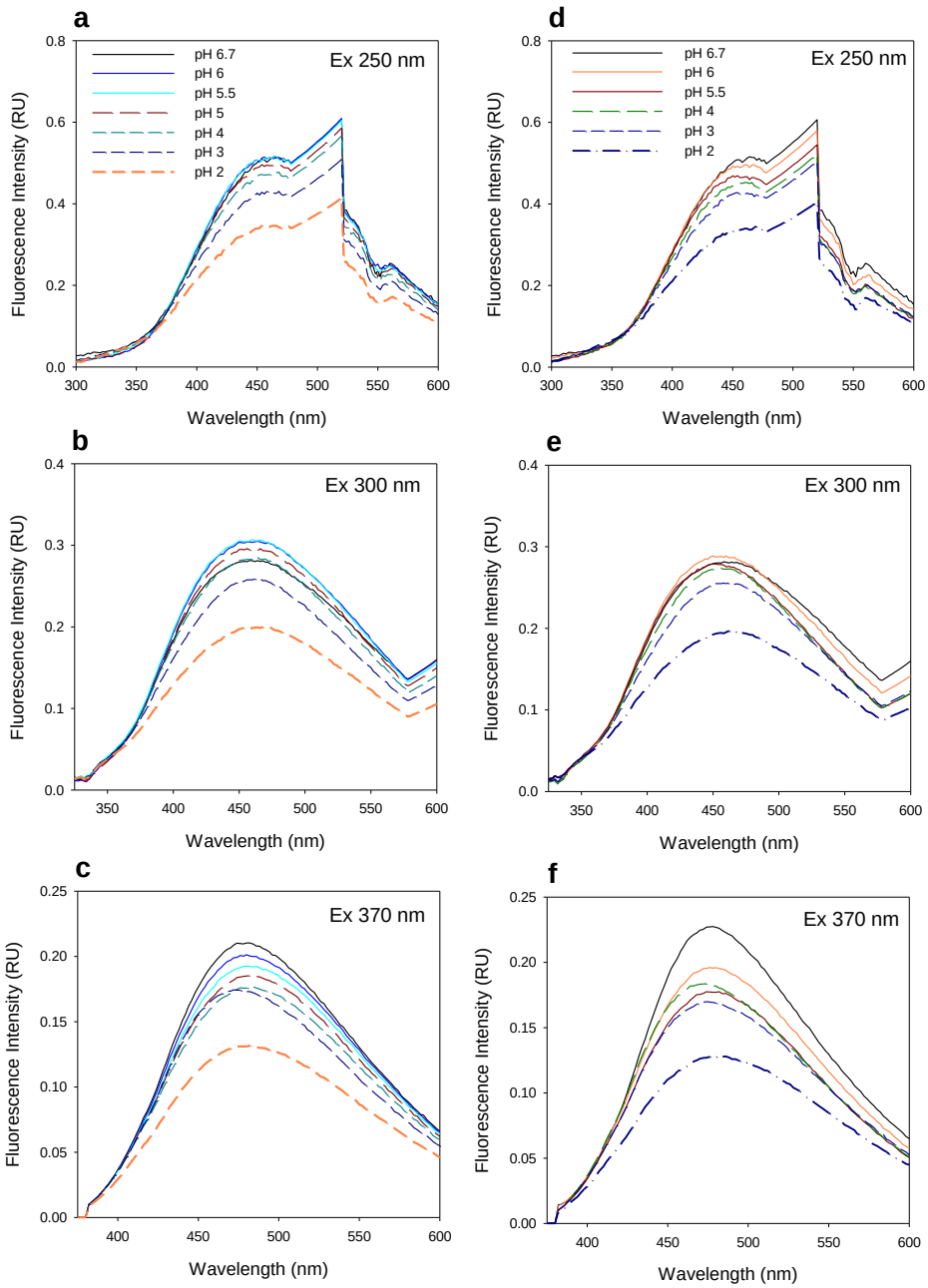

Figure A- 8. 2D fluorescence emission spectra of Suwannee River HPoA in the absence (left panel) and presence (right panel) of 0.68 mg L^{-1} iron at excitation wavelength 250, 300 and 370 nm between pH 2 and 6.7. pH 5.0 spectra of iron containing solutions omitted due to deviation from target pH.

CHANGES IN THE FLUORESCENCE INDEX BY IRON

Changes in the FI values defined as emission ratio 450 to 500 nm proved less vulnerable to interference by iron than those defined at emission ratio 470 to 520 nm. The most pronounced difference was observed in the Everglades F1 HPoA, where increases in FI (450 nm to 500 nm ratio) at high iron:DOC did not exceed 0.03 FI units regardless of oxidation state. Changes in Suwannee River HPoA FI values were slightly less at 0.06 FI units for both iron(II) and iron(III) when determined at emission 450 to 500 nm. Williams Lake water and Everglades F1 water had comparable, but small, changes in FI regardless of fluorescence emission ratio. The wavelength of peak emission at excitation 370 nm was determined for all samples. No significant blue shift (≤ 4 nm) in peak emission wavelength was observed in all samples due to iron or pH effects, which has been observed in the presence of other metals (Senesi, 1990; Provenzano et al., 2004). These results provide evidence that observed changes in FI values are a product of subtle fluctuations in the slope of the emission 370 nm peak, which draws attention to the sensitivity of indices based on excitation/emission wavelengths pairs sensitive to subtle changes in solution chemistry. A recommendation on fluorescence region(s) more conservative to changes in sample chemistry is withheld due to observations of variable iron-quenching behavior across samples of differing DOM composition. Although variable in significance between sample replicates, the acidification of Suwannee River HPoA showed higher FI values are pH 3. EEMs presented in Figure 9 show a distinct fluorescence reduction at high excitation/emission wavelengths, which may explain this behavior.

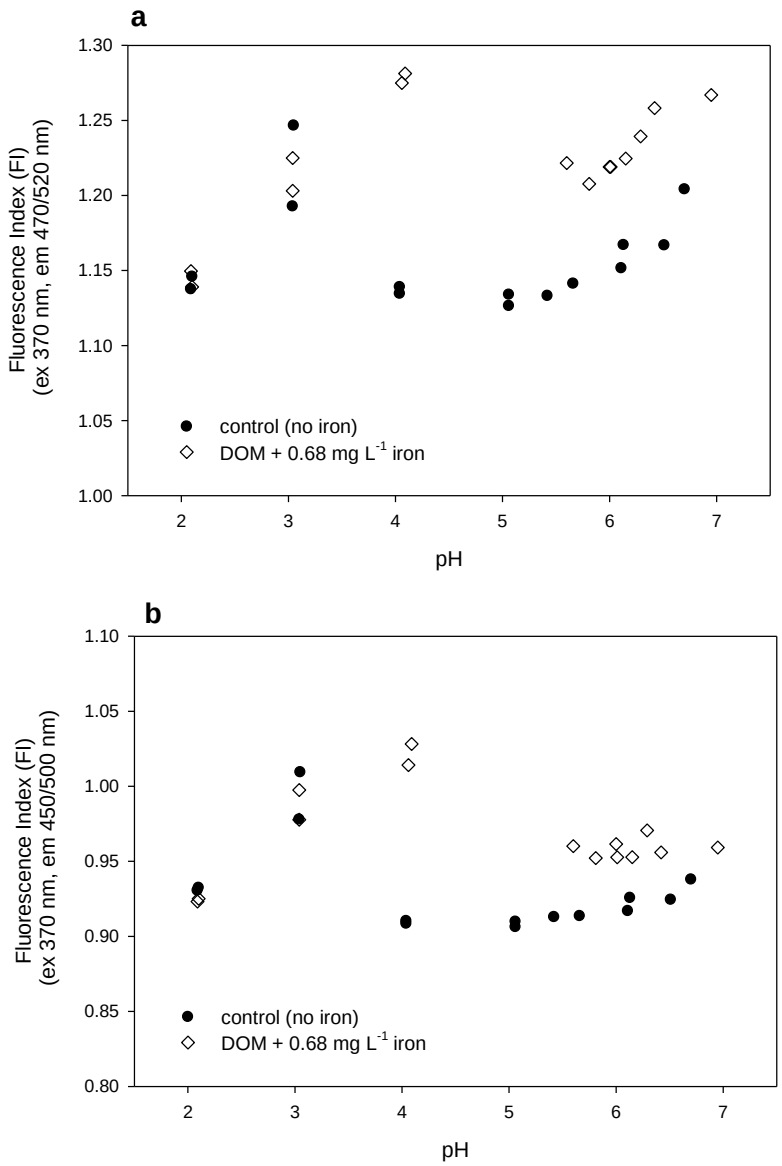

Figure A- 9. Changes in fluorescence indices determined at emission ratio (a) 470 and 520 nm and (b) 450 and 500 nm of excitation wavelength 370 nm of Suwannee River HPoA in the absence and presence of 0.68 mg L^{-1} iron added as iron(II).